Journal of Thermal Biology 84 (2019) 292–310

Contents lists available at ScienceDirect

Journal of Thermal Biology

journal homepage: www.elsevier.com/locate/jtherbio

# Aquatic animal colors and skin temperature: Biology's selection for reducing oceanic dolphin's skin friction drag

M. Hassanalian[a,*], H. Abdelmoula[b], S. Mohammadi[c], S. Bakhtiyarov[a], J. Goerlich[d], U. Javed[e]

[a] Department of Mechanical Engineering, New Mexico Tech, Socorro, NM, 87801, USA
[b] Gowell International, LLC, Houston, TX, 77041, USA
[c] Department of Biotechnology, New Mexico Tech, Socorro, NM, 87801, USA
[d] Forum Energy Technologies, Houston, TX, 77041, USA
[e] Engineering Department, American University of Iraq, Sulaimani, Kirkuk Rd, Sulaimania, 46001, Iraq

ARTICLE INFO

*Keywords:*
Orca
Dusky dolphin
Turbulent flow
Irradiation
Drag
Energy balance

ABSTRACT

There is currently a growing interest in the area of drag reduction. In this work, the thermal effects of body color of some species of aquatics like Orcas and Dusky dolphins are investigated with respect to their swimming routes and geometric and behavioral characteristics. Considering the marine and atmospheric characteristics of these aquatics' routes, a thermal analysis is performed. The surrounding fluxes including the water flux, sun irradiation, and core temperature are considered in an energy balance to determine the skin temperature of the top side of the animal/organism's body. To study the effects of color on the surface temperature of the aquatic species, an experiment is carried out in the water on a flat plate with black and white color. Applying a turbulent analytical solution for heated boundary layers, it will be shown that the black color on the top of the bodies of these marine organisms is very efficient in terms of skin drag reduction. Moreover, to investigate the effects of the temperature on underwater skin friction drag reduction, the turbulent flow is simulated around a flat plate and a 2- dimensional modeled Killer whale at different temperatures. The results show that the top black body color of Orca and Dusky dolphin decreases their skin friction drag by 7%. This study will also provide the reason for this evolution of color scheme of other extremely fast marine animals, such as billfish, whales, and sharks. This method of drag reduction can be considered as one of the effective factors in skin drag reduction of underwater robots.

## 1. Introduction

With the present energy crisis around the world, there is an ever-increasing need of research for drag reduction and performance enhancement techniques (Mirzaeinia et al., 2019). Since nature has developed processes, objects, materials and functions to increase efficiency, it has the best answers when we seek to improve or optimize a system (Hassanalian et al., 2017a). Thus, the fields of biomimetics and bioinspiration allow us to mimic biology or nature to develop methods for reducing drag in all types of transportations involving land, sea, and air (Bushnell and Moore, 1991). Swimming under the water, a characteristic adaptation of natural aquatics, such as fishes, rays, whales, and other biological animals, is considered one of the most demanding adaptations in nature owing to the physical challenge of motion in water (Helfman et al., 2009). Being the most ancient multicellular animals on Earth, the aquatics benefit from 500 million years of evolution enabling them to develop adequate anatomy to interact with the environment in an optimal way (Valentine, 1978). For example, aquatic animals have gradually shaped into various excellent structures by adopting their movement modes like oscillation or undulation, and hence taken advantage of their motion in an underwater environment (Bushnell and Moore, 1991). This continual tendency to improve themselves has a history that has undergone millions of years of natural selection.

The advent of recent technologies enables researchers to understand animals' forms and their functions accurately and improvise their behaviors to come up with optimized engineering systems. In the underwater environment, each type of aquatic animal has its own characteristic way of motion that suits its own food chain and needs. The speed and movement characteristics of these animals are generated by various means; flexible bodies and fin structures in fishes, or a form of jet propulsion in aquatics like octopus or jellyfish (Fish, 2013). These different solutions increase their maneuverability and swimming capabilities for their respective needs. Therefore, biologists and engineers

* Corresponding author.
*E-mail address:* mostafa.hassanalian@nmt.edu (M. Hassanalian).

https://doi.org/10.1016/j.jtherbio.2019.07.018
Received 27 May 2019; Received in revised form 14 July 2019; Accepted 14 July 2019
Available online 15 July 2019
0306-4565/ Published by Elsevier Ltd.

see aquatic animals as a reference when making an optimized underwater engineering system (Vincent and Mann, 2002).

Different mechanisms are employed by biological aquatic systems for performance enhancement and drag reduction. Generally, there are three types of drag in nature which include skin-friction drag, shape drag, and drag due to the lift for organisms/systems totally immersed in a fluid, whether air or water (Bushnell and Moore, 1991). The generated drag by biological aquatics varies in accordance with different factors, such as flow conditions around the organism and in its boundary layer, as well as proximity to the air-water interface. Different strategies and mechanisms are employed by marine organisms to decrease the aforementioned drags (Bushnell and Moore, 1991). These mechanisms that reduce the drag under water include anatomical and physical features, secreted materials and behavioral patterns. For instance, in marine organisms, the mucus covers the living fishes' surface and reduces friction drag (Hoyt, 1975). Similarly, sharks have riblets which are streamwise microgrooves in their bodies (Martin and Bhushan, 2014). Also, viscous and dynamic damping are employed by biological aquatics to effectively reduce friction drag (Ahlborn et al., 2009). Boundary layer acceleration is another mechanism which is employed by organisms, such as whales by injecting high momentum fluid into their boundary layer and can delay both transition and separation, consequently reducing the friction drag (Fish, 2006) (Bushnell and Moore, 1991).

One of the other methods in drag reduction applied by warm-bloodied aquatics, such as marine mammals and scombrid fishes is boundary layer heating (Bushnell and Moore, 1991). These organisms have the capacity to use heat conducted from the body surface to decrease water viscosity around their body and consequently reduce the drag. It was investigated by Hassanalian et al. that the black and white colors of migrating birds' wings, such as albatrosses can have an effect on their skin drag reduction (Hassanalian et al., 2017b). In this study, the migration routes of birds with black and white colors, including the latitudes and longitudes, the time of migration, and the corresponding marine and atmospheric characteristics, such as wind speed, ambient temperature, ocean temperature and sky temperature of their flight routes were investigated (Hassanalian et al., 2018a). The thermal effects of the top side and bottom side of the wing with two different colors (white and black) have been studied. Using the Blasius boundary condition, it was shown that the boundary layer around the wings of the birds with black color on top have less density and more viscosity than white color (Hassanalian et al., 2018a) (Hassanalian et al., 2018b). In other words, for the dark colors, there is an increase in the wing surface temperature and therefore a corresponding decrease in the density and an increase in the viscosity, but the total skin drag decreases.

In this work, a new factor, which is affecting the boundary layer of some aquatics and subsequently their skin drag reduction, is studied. One of the main aspects, which are remarked in a couple of Epipelagic Zone animals, is the black skin on the upper area. The thermal effects of body color of marine organisms are investigated in some species, such as whales, manta rays, dolphins, penguins, sharks, seals, and billfish that have black color on the top, and white color on the bottom sides of their respective bodies. As examples, Orcas and Dusky dolphins are considered for a full analysis in order to investigate their colors' effects.

The main objective of this study is to investigate the functional significance of aquatics' body colors under the assumption that it is optimally adapted and propose the best colors for underwater robots to decrease their drag forces and increase their endurance. The rest of this paper is organized as follows. The heated boundary layer and drag reduction in aquatics are discussed in section 2. In section 3, characteristics of the organisms and their environment are presented. Experimental thermal study on flat plates with black and white color, and modeling, energy balance, and governing equations are shown in sections 4 and 5, respectively. The calculation of skin friction drags for Orcas and Dusky dolphins with black and white colors, theoretically and computationally are indicated in sections 6, 7, and 8 respectively. Summary and conclusions are given in section 9.

## 2. Heated boundary layer and drag reduction in aquatics

From a fluid dynamics perspective, it was reported on multiple occasions that an increase in temperature might result in an improvement of fluid performance like the delay of the turbulent region and a reduction in the vortex shedding. However, one of the most noticeable improvements is the decrease of the skin drag across solid surfaces. Li et al. proved that an increase of 20 °C in temperature of water decreases the skin friction in a turbulent flow. Their numerical model proved that this change is basically due to the decrease in Reynolds shear stresses near the boundary layer (Li et al., 2004). Peeters et al. showed that an increase in temperature at 0 °C will contribute towards decreasing the density and viscosity of the water which leads to suppression of vortices near the wall. The absence of these vortices reduces the energy dissipated across the boundary layer (Peeters et al., 2016). Finally, Cho et al. proved that an increase in temperature plays a key factor in flow drag reduction. They proved that at low temperatures the concentration of non-ionic surfactants does not decrease the drag as efficiently, compared to high temperatures (Cho et al., 2007). This can be related to Highly Migratory Species (HMS) such as the aforementioned billfish among others. The common trend among these pelagic fish is that they are colored in such a way that it benefits their survivability. For fish that fall into the HMS category, one notable survivability characteristic is their ability to swim long distances that can be directly related to their achievable speed. Swordfish are an HMS which have multiple genetic characteristics that can be seen to be temperature dependent. The bulk of their skin's surface area is a dark blackish-blue, most notably their fins which support the reduction of skin drag by increasing skin temperature. Additionally, a secondary benefit of higher temperature was noted by Fritsches et al. that the swordfish retina was sensitive to temperature change and showed an increase in flicker fusion frequency from 5 Hz to 40 Hz during a temperature change from 10 °C to 20 °C, respectively (Fritsches et al., 2005).

Expanding beyond billfish species, the predatory fish within the HMS category, such as *Coryphaena hippurus*, or more commonly referred to as Dolphinfish or Mahi-Mahi, have been noted to change their colors under various conditions. Murchison and Magnuson noted their color would change between a silver-blue and a yellowish phase. The yellowish phase was reported to come out or be more pronounced when it was reacting to a feeding frenzy or struggling on a fisherman's hook. This can be related to their ability to swim faster by darkening their color to reduce skin drag (Murchison and Magnuson, 1966).

In this work, considering the marine and water characteristics of the mentioned species, such as Orcas and Dusky dolphins, a thermal analysis will be performed when these aquatic animals are in motion, under and over the water. The surrounding fluxes including the water flux and the sun irradiation are considered in an energy balance to determine the skin temperature of top side of the animal/organism's body. For the considered aquatic structures, the 1/5 power law boundary layer, will be used to determine an analytical expression of the skin drag. Applying the analytical solution for turbulent heated boundary layers, it will be shown that the black color on the top side of the bodies of these marine organisms is very efficient in terms of skin drag reduction. This study will also provide the reason for this evolution of color scheme of these extremely fast marine animals, such as billfish, whales, dolphins, and sharks. This method of drag reduction can be considered as one of the effective factors in a skin drag reduction of underwater robots.

## 3. Characteristics of black and white aquatics and their environments

In this study, aquatics like Orcas and Dusky dolphins as the fastest marine organisms with a dark color on the top and white color at the bottom side of their bodies are considered.

**Table 1**
Geometrical and swimming characteristics of aquatics with black and white colors.

| Aquatic | Length (m) | Core temperature ($^{O}$C) | Weight (kg) | Swimming speed (km/h) |
|---|---|---|---|---|
| Killer whale | 5–9.8 | 36–38 | 3000–10000 | 56 |
| Dusky dolphin | 1.7–2.1 | 36–37 | 69–100 | 37 |
| Manta rays | 5.5–6.7 | 20 | 1400 | 24 |
| Sharks (Blacktip Reef) | 1.5–1.9 | 14–27 | 20–25 | 96.5 |
| Sailfish | 1.2–3 | 26.8 | 90 | 36–54 |

**Fig. 1.** Marine organisms with black and white colors.

**Orca:** The *Orcinus orca*, also known as Orcas or killer whales, belong to the Oceanic dolphin family, of which it is the largest member, and they are classified in four different types namely A, B, C, and D (Ford, 2009). Type A Orcas that are living in open water, look like typical Orcas and have black-and-white form with a medium-sized white eye patch. Type B Orcas are smaller than type A and most of the dark parts of their bodies are medium gray instead of black, although they have a dark gray patch called dorsal cape. Type C Orcas are the smallest and live in larger groups than others. These type of Orcas like type B have primarily white and medium gray, with a dark gray dorsal cape and yellow-tinged patches. Types B and C Orcas generally are living close to the ice pack and diatoms in these waters may be responsible for the yellowish coloring of both types. Typical Orcas usually have a black back, white chest and sides, and a white patch above and behind their eyes (Pitman and Ensor, 2003) (Pitman et al., 2007). Orcas are considered as the largest aquatics. Males typically range from 6 to 8 m long and weigh in excess of 6000 kg and females generally range from 5 to 7 m and weigh about 3000–4000 kg. The largest male and female Orcas on the record are 9.8 m weighing 10000 kg, and 8.5 m weighing 7500 kg, respectively (Dahlheim and Heyning, 1999). The Orcas are among the fastest marine mammals, able to reach speeds in excess of 56 km/h and their mean core temperatures are 36–38 °C (Dahlheim and Heyning, 1999) (Kasting et al., 1989). Orcas evidently prefer high latitudes and coastal areas, to pelagic environments including the coasts of Iceland, Norway, Valdes Peninsula of Argentina, Crozet Islands, New Zealand and parts of the west coast of North America, from California to Alaska (Baird and Baird, 2006). It should be noted that the Orcas spend the vast majority of their time (> 70%) in the upper 20 m of the water column (Mann et al., 2000).

**Dusky dolphin:** The Delphinidae, also known as Oceanic dolphin, not to be confused with porpoises, are a widely distributed family of dolphins that live in the sea and range in size from 1.7 to 9.4 m long and 50–10000 kg weight. Some of the dolphins can travel at speeds up to 55.5 km/h (Macdonald, 1995). Oceanic dolphins are widespread, but most species prefer the warmer waters of the tropical zones (Hastie et al., 2005). Most dolphins, such as long-beaked common dolphin and Dusky dolphin have dark gray or black color in their back and white chest (Stevens and Merilaita, 2011). The dusky dolphins are smaller compared with other species of dolphins. These aquatics have a length range of 1.7–2.1 m and a weight range of 69–100 kg. Most of the dolphins generally live in fairly shallow waters and spend a considerable amount of their travel time close to the water surface. In other words, they are partially submerged or fully submerged in water but close to the surface. These aquatics are close to the surface within 5 m as they do breathe oxygen and the farthest this species has been noted is approximately 130 m. In general, the depth at which these dolphins may swim can vary (Wiirsig et al., 1991).

**Manta rays:** One unique class of aquatics that combines undulation with oscillation is the Rajiform. Rajiforms are rays; these animals have enlarged pectoral fins and have a spectrum of swimming styles (Last et al., 2016). Rays species that display these two fin-swimming styles more distinctly are the manta ray with oscillatory flapping and the stingray with undulatory motion (Klimley, 2013). The fins of manta rays are capable of large deformation amplitudes with periods less than one. From a top-down view, the manta ray has triangular shaped fins. Rays are capable of large fin deformations because their bodies do not have bony structures; they are pseudo rigid cartilage structures (Fish et al., 2016). These are described as rib-like skeletal structures and are cross weaved in the fin. Complex musculature pulls on these cartilage ribs, causing flexion to the fin. Manta rays alter left or right fin

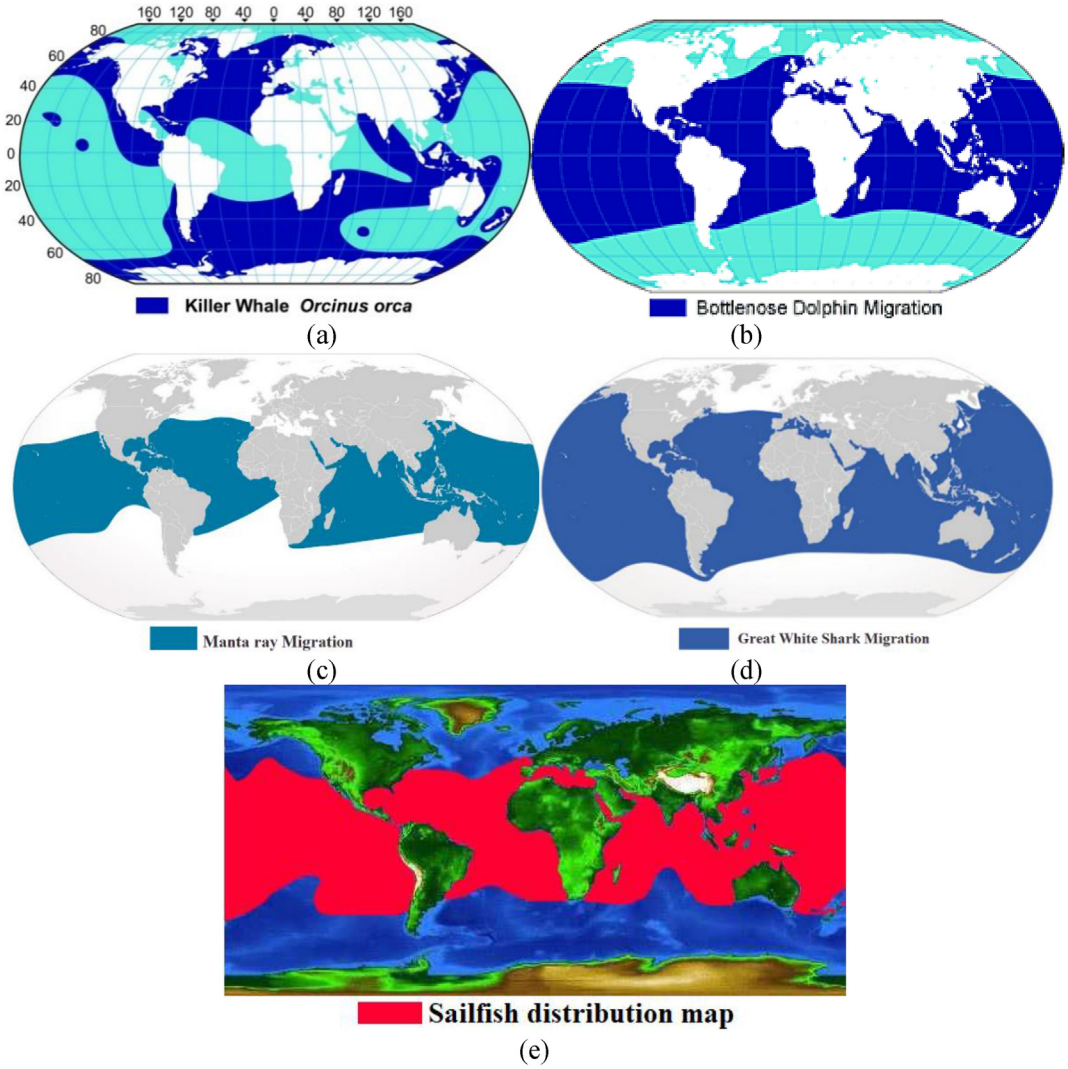


**Fig. 2.** View of migration range and distribution map of (a) killer whales (American Cetacean Society, 2013), (b) Oceanic dolphins (American Cetacean Society, 2017), (c) manta rays (Wikipedia, 2012), (d) great white sharks (Rogers, 2019), and (e) sailfishes (Gardieff, 2017).

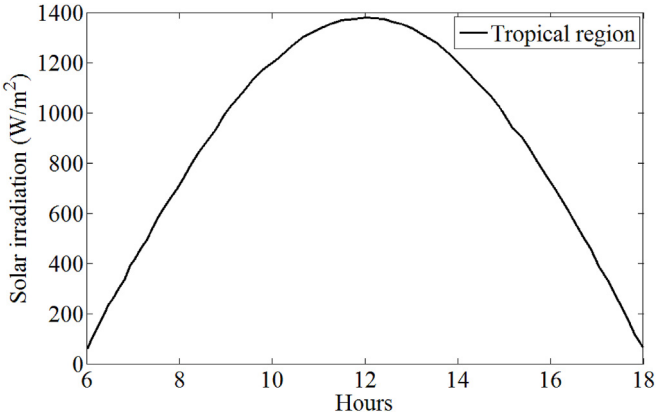


**Fig. 3.** View of solar irradiation for tropical regions (Handara et al., 2016).

amplitude to make turns. Manta rays are such large rays that they have a width in the range of 5.5–6.7 m which is about 2.2 times the length of their bodies. Manta rays are quite heavy and, in some species, can reach 1400 kg and have a swimming speed of 24 km/h (Dewar et al., 2008). These types of aquatics are found in warm temperate, subtropical and tropical waters and prefer water temperatures above 20 °C (Ebert, 2003). They typically have black or dark color on the top part and white or pale color on the bottom sides of their bodies (Marshall et al., 2009). Mantas sometimes breach; leaping partially or entirely out of the water. The reason for breaching is not known for manta rays (Deakos, 2010).

**Sharks:** There are varieties of sharks that have different characteristics. For example, Blacktip Reef is considered small but lightning fast that have a length of 1.5–1.9 m and a weight of 20–25 kg. This species generally can be found in the warm and shallow water near sandy beaches and coral reefs. Most of the sharks typically have dark color on the upper side and bright color on the bottom side of their bodies. Sharks are considered as the fastest aquatics and in some species can reach up to speeds of 26.8 m/s (Gibson, 2002).

**Sailfish:** Sailfish is one of the organisms that are predominantly blue to gray in color, grow quickly and have a length of 1.2–1.5 m in a single year. Generally, sailfish do not grow to more than 3 m in length and rarely weigh over 90 kg. Sailfishes have speeds between 10 and 15 m/s and swim near the water surface (Marras et al., 2015) (Svendsen et al., 2016). The geometrical and swimming characteristics of the considered aquatics including Killer whale, Dusky dolphin, manta rays, sharks, and sailfish are shown in Table 1. The geometrical and swimming characteristics of the mentioned aquatics and views of their black and white colors are shown in Table 1 and Fig. 1, respectively.

The swimming areas of these aquatics are as follows. The Orca or Killer whales, unlike other HMS, are not following a yearly migration

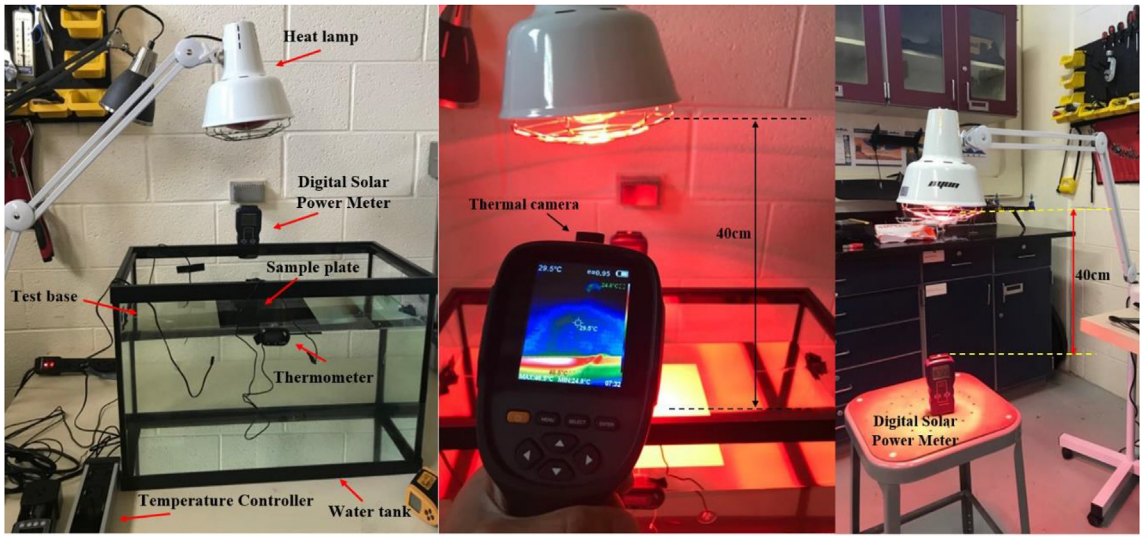


**Fig. 4.** Experimental setup to study the color effects on surface temperature.

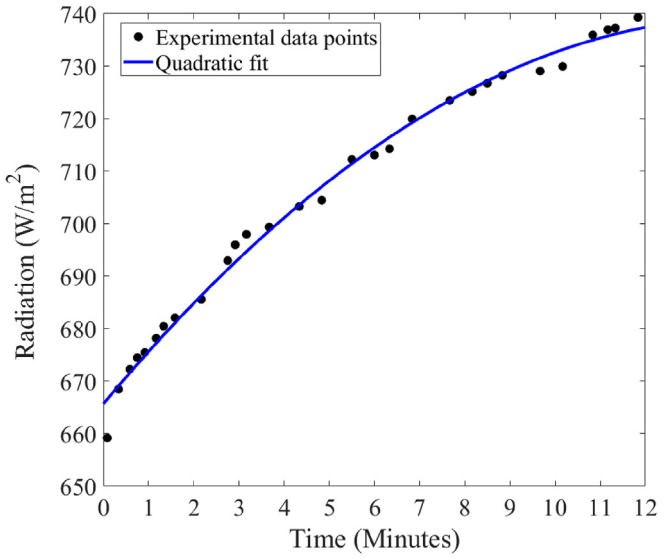


**Fig. 5.** Radiation versus time for heat lamp with 40 cm distance from the plate.

route at all. Instead, they can be seen within the majority of the world's oceans and are one of the most widely distributed animals on Earth (Ford, 2009). This type of HMS travels freely throughout their range, following their food. In Fig. 2(a), a view of their range is shown. As can be seen in Fig. 2(a), the Orcas' habitat extends from the icy polar oceans to the warm waters of the tropics. These Orcas spend most of their time in the open ocean as well as in more shallow coastal waters (Baird and Baird, 2006).

Oceanic dolphins live in temperate and tropical waters throughout the world extending from deep ocean waters to harbors, lagoons, bays, gulfs, and estuaries (Mann et al., 2000). The coastal ecotype of dolphins is generally adapted for warm and shallow waters as their smaller body and larger flippers increase their heat dissipation and maneuverability. In contrast, the offshore ecotype of dolphins is typically adapted for cooler and deeper waters. They have a larger body that helps conserve more heat and defend against predators. Most dolphins experience seasonal movements, probably as a response to variations in migration of fish and water temperature (Mann et al., 2000) (Wiirsig et al., 1991). In Fig. 2(b), a view of the dolphin's migration range is indicated.

Since manta rays prefer warmer waters, they are living typically in the tropical and subtropical oceans. Manta rays have been seen in the water range from North Carolina in the United States (31°N) to New

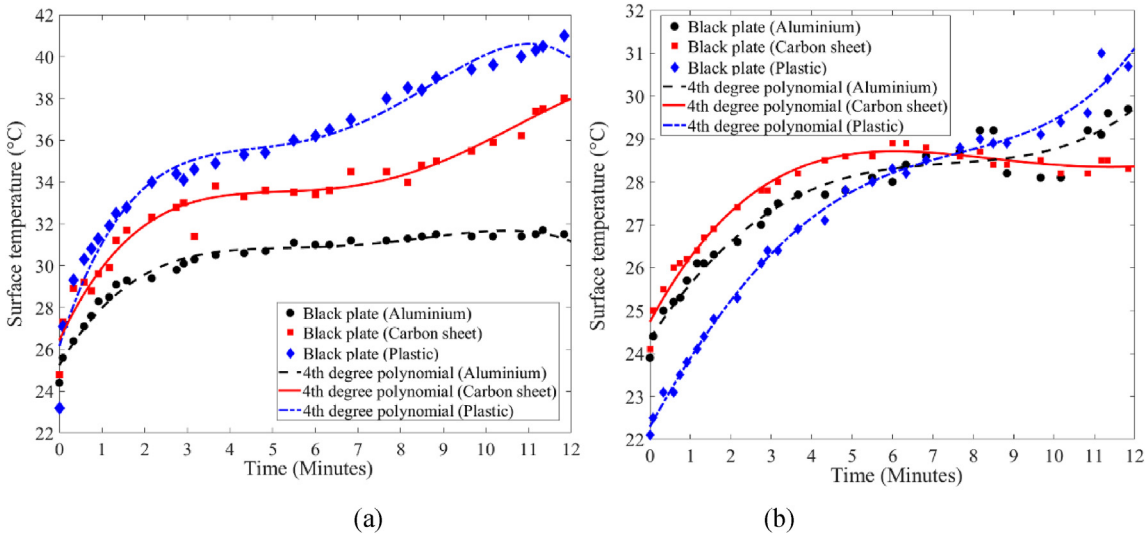


**Fig. 6.** Surface temperature versus time for aluminum, carbon, and plastic black plates (a) inside and (b) outside of the water.

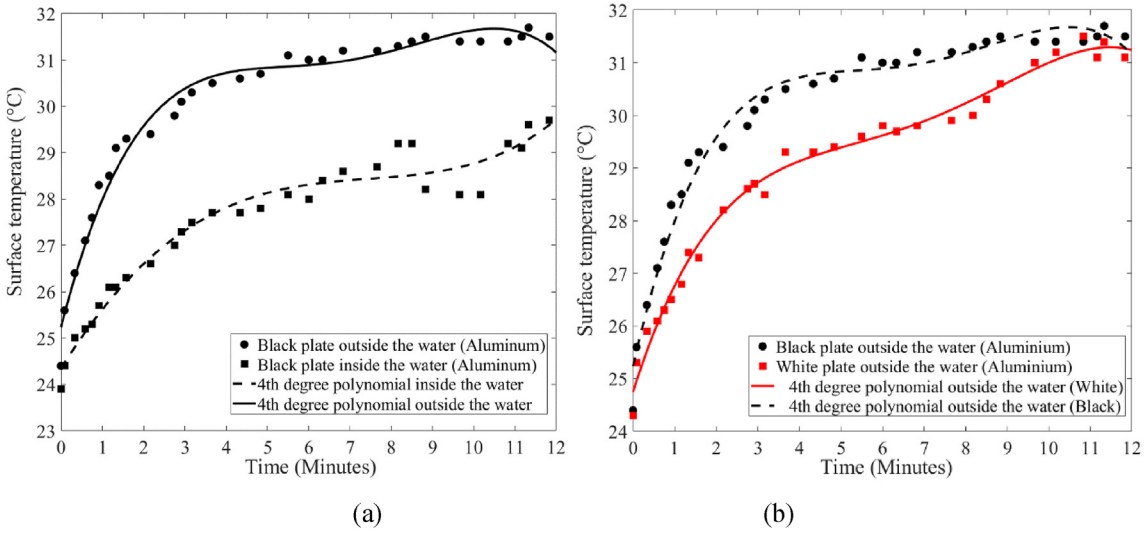


**Fig. 7.** Surface temperature versus time for (a) black plate inside and outside of the water, and (b) black and white plates outside the water.

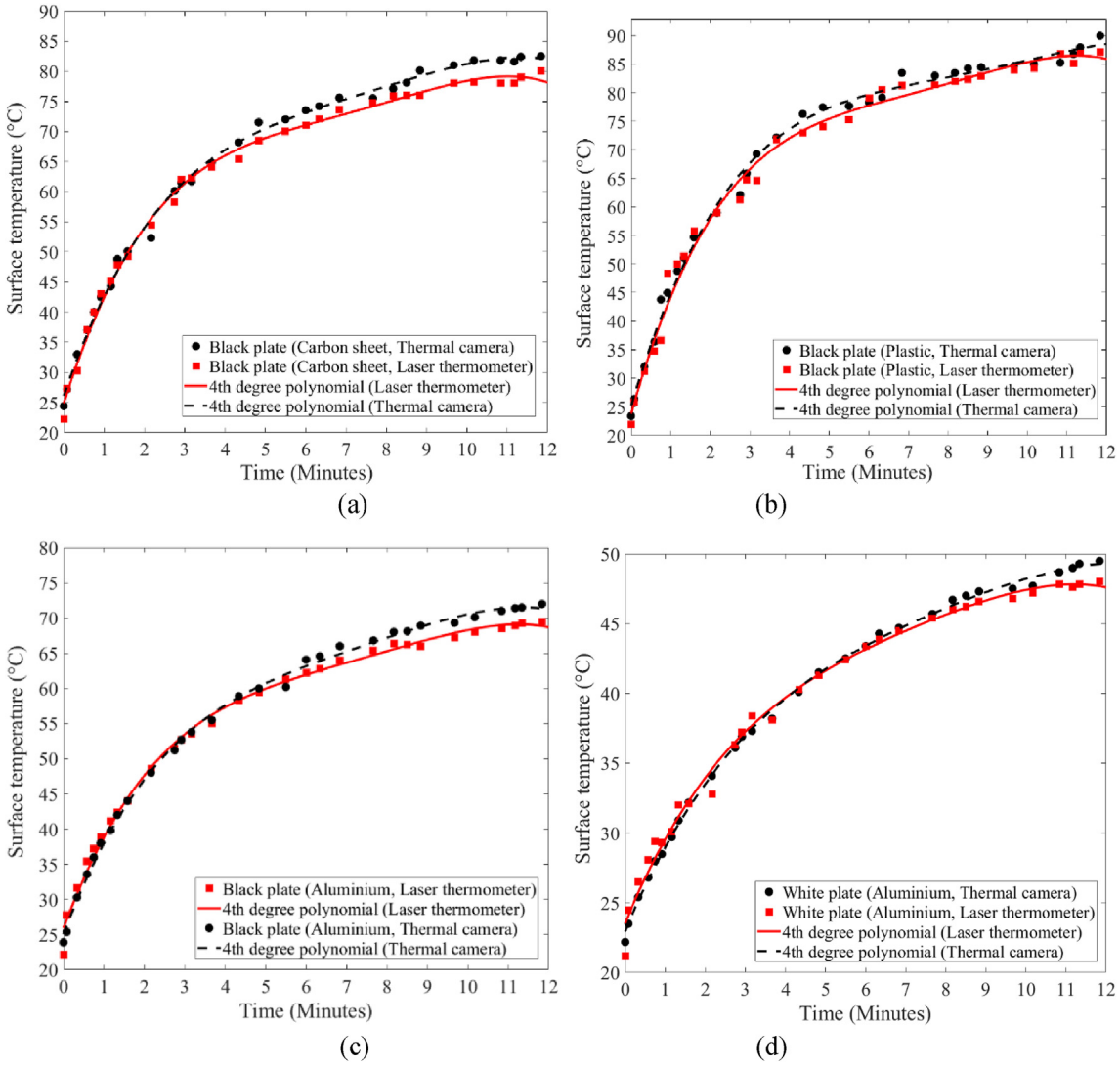


**Fig. 8.** Surface temperature versus time for (a) black carbon plate, and (b) black plastic plate, (c) black aluminum plate, and (d) white aluminum plate on a wood-base.

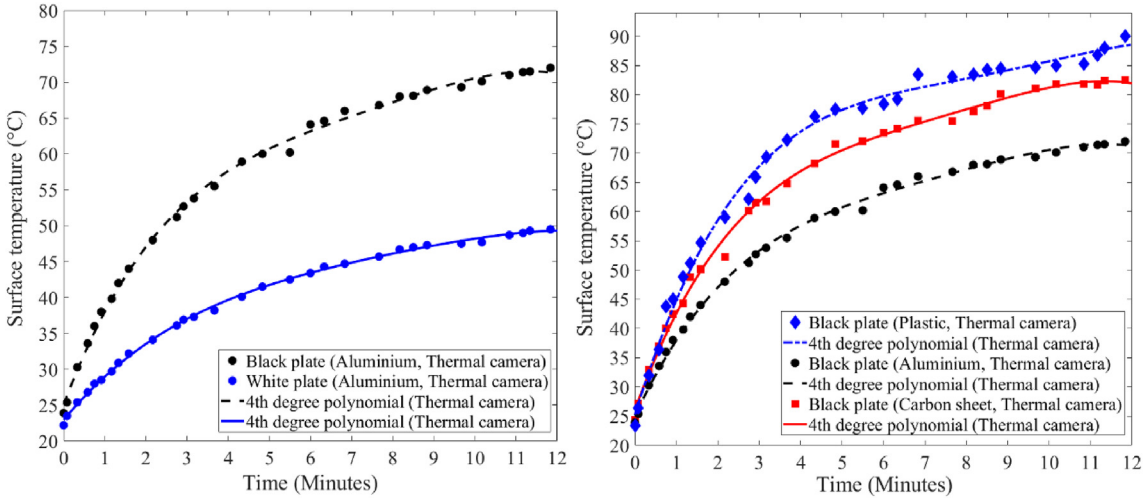


**Fig. 9.** Surface temperature versus time for wood-base aluminum black and white plates.

Zealand (36°S). These aquatics generally only venture into temperate seas when the water temperature is at least 20 °C. Manta rays are common in coastal waters from spring to fall, migrate as far as 1000 km and occur at depths ranging from sea level down to 1000 m (Last et al., 2016) (Klimley, 2013). During the day, manta rays swim near the surface and at night, they venture deeper (Ebert, 2003). In Fig. 2(c) a view of the manta ray migration route is shown.

As mentioned above, there are different types of sharks, but great white sharks, which have dark color on the top of their bodies, are considered in this study. Although great white sharks prefer the coastal areas in all oceans from all over the world, they typically live on the outskirts of shore waters. Sometimes, they dive into the deep ocean and are even found in depths of 1000 m or more. However, their preferred water temperature is from 15 to 24 °C, so most of the time they stay in shallow waters and near the surface (Ebert, 2003) (Gibson, 2002). In Fig. 2(d), the habitats of the great white sharks are shown.

The sailfish can be found from approximately 40° N to 40° S in the western Atlantic Ocean and from 50° N to 32° S in the eastern Atlantic Ocean (Marras et al., 2015). They also have been seen in the Mediterranean Sea, although few records exist for this region. For example, Atlantic sailfish are typically found in tropical regions and temperate waters of the western Atlantic from the Gulf of Maine south to Brazil, including the Caribbean and the Gulf of Mexico (Lam et al., 2016) (Kerstetter et al., 2011). In this region, the distribution of these fishes is apparently influenced by water temperature as well as wind conditions. These type of fishes generally migrate throughout the mentioned range and stay at the depths above the thermocline, in water temperatures between 21 and 28 °C (Lam et al., 2016). Sailfish generally appear during warm seasons, to this end, the seasonal changes will affect these aquatics' distributions. In the Pacific Ocean, the sailfish are commonly found in temperate and tropical regions. These fish exist in waters from 45° to 50° N to 35° S in the western Pacific and from 35° N to 35° S in the eastern Pacific (Ehrhardt and Fitchett, 2006) (Lu et al., 2015). Sailfish are found in abundance, especially in Papua New Guinea and Philippines, as well as from Tahiti to Marquesas and Hawaii. This species can also be found in the Indian Ocean to approximately 35–45° S latitude (Gardieff, 2017). In Fig. 2(e) a view of the distribution map for the sailfish is shown.

After determination of the range of the considered aquatics, the marine and atmospheric characteristics of the corresponding environments are extracted. The effective parameters in this study are sky temperature, ambient air temperature, ambient water temperature and solar irradiation which are specified for each range of migrating aquatics. Ambient temperature is crucial to understand the energy balance in considered aquatics. In such oceanic locations, it is hard to determine the air and water temperature every hour. For this work, an average value is considered for ambient air temperature in tropical regions. Implementing the ambient temperature in Eq. (1), the effective sky temperature $T_{sky}$ can be obtained as follows (Adelard et al., 1998):

$$T_{Sky}^4 = T_a^4(1 - 0.261\exp(-7.77 \times 10^{-4})(T_a - 273)^2) \quad (1)$$

The average ambient temperature of the ocean surface waters is about 16.1 °C. The hourly radiation received by the Earth in the tropical region is shown in Fig. 3.

## 4. Experimental thermal study on flat plates with black and white color

In order to investigate the effects of the colors on surface temperature, an experiment is designed in the laboratory. Two aluminum flat plates with black and white colors are set up on top of a water tank. Two different cases are studied during the experiment. In the first case, the flat plate will be floated over the water and in the second case, the flat plate will be placed close to the water surface in such a way that a thin layer of the water will cover the top. We ensured during experiments that plate is partially submerged or fully submerged but at the surface; exactly the same configuration that a Dusky dolphin exhibits during its motion in migration. The Orcus/Killer whales use same strategy of staying close to surface of water as well during long journeys. To check and control the ambient water temperature, a thermometer and two temperature-controllers are installed inside the water tank, respectively. A heat lamp at 40 cm from the plate is used in this experiment to provide and simulate the sun irradiation. The two aluminum plates with black and white colors are exposed to the heat lamp for 12 min, and their surface temperatures are measured by a thermal camera and laser thermometer. To measure the irradiation of the heat lamp, a SM206 Digital Solar Power Meter Sun Light Radiation Measuring Testing Instrument is used. In Figs. 4 and 5, the designed experimental setup and the measured radiation from the heat lamp are shown, respectively.

It is important to note here that the main objective behind the experiment is to put into consideration the effect of the color due to radiation effects and to have them corroborate with the considered heat equation results in the next section. Therefore, unidirectional movement and/or side to side movement effects of considered flat plate are not considered as the efficacy of color effects would come out to be pronounced even with the simple experimental setup utilized. While it would be interesting to represent in terms of dynamic temperature analyses for any aquatic species, this particular experiment takes a simplified approach for studying the effect of one attribute of the

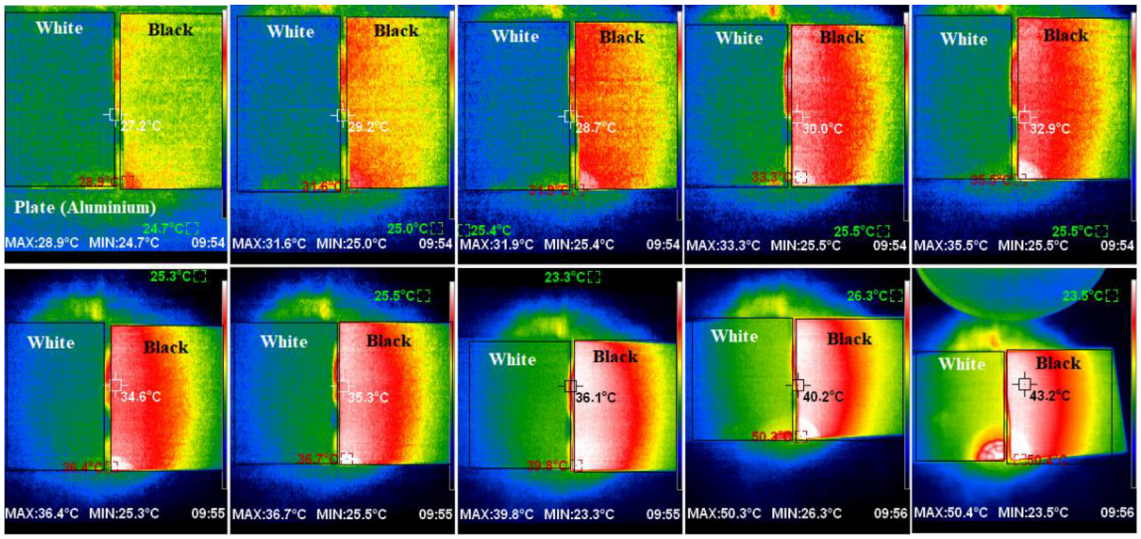


(a)

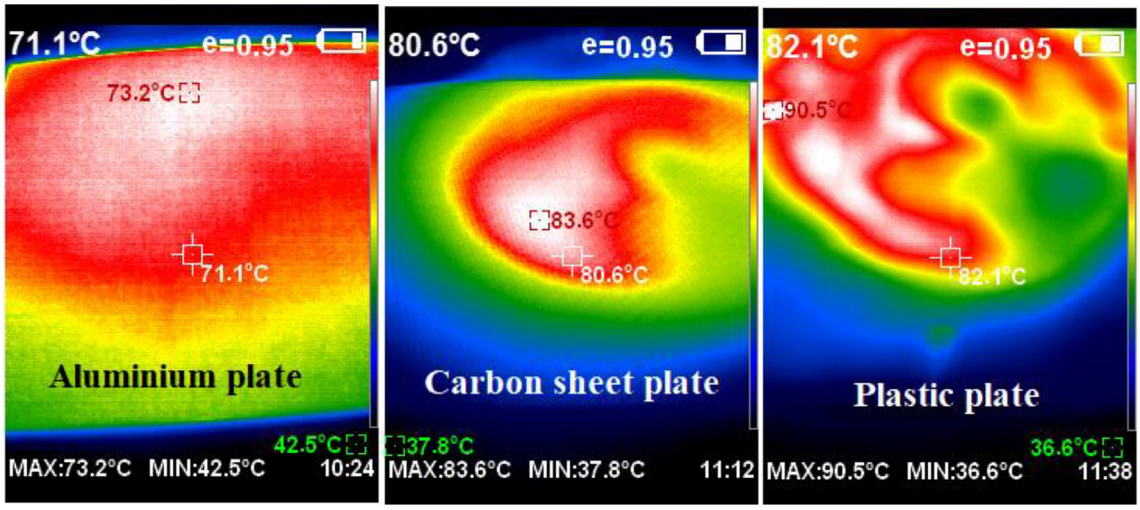


(b)

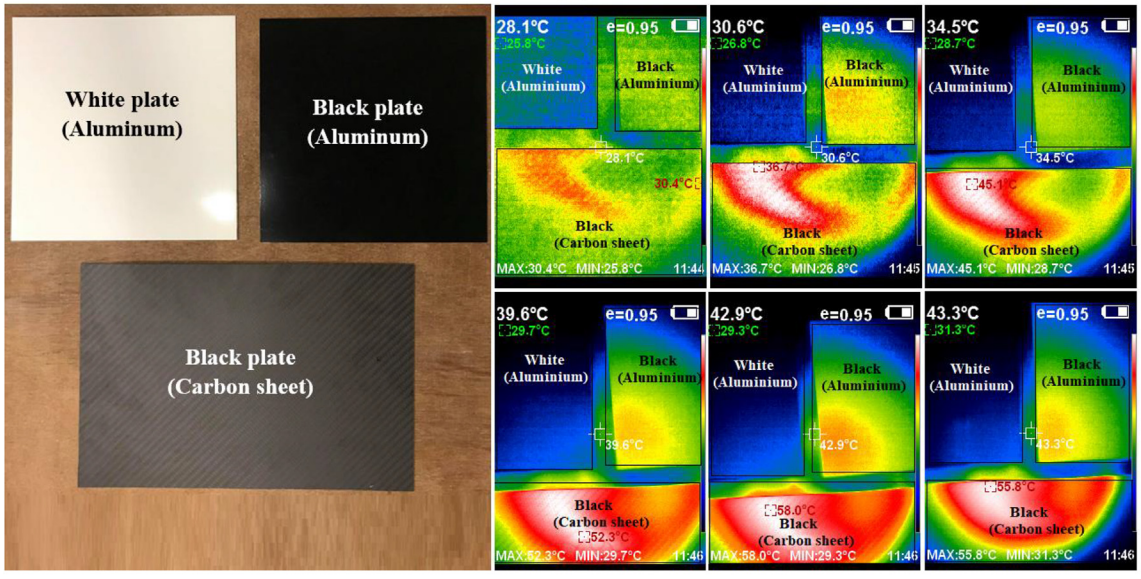


(c)

**Fig. 10.** Surface temperature distribution for (a) black and white aluminum plates, (b) black plates from aluminum, carbon, and plastic, and (c) white and black aluminum, and carbon plates with a wood-base.

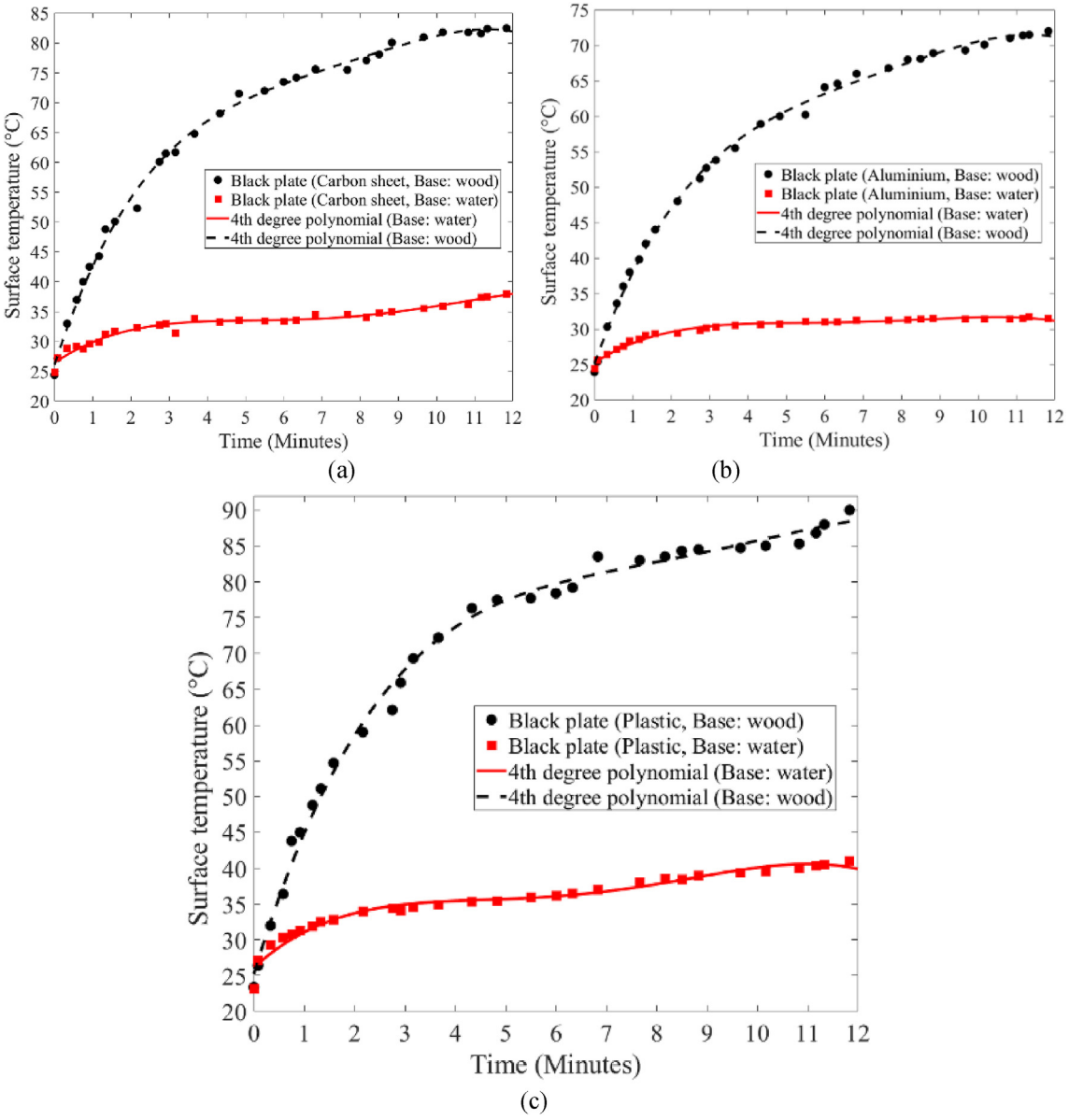


**Fig. 11.** Surface temperature versus time for black (a) carbon, (b) aluminum, and (c) plastic plates with a water and wood-base.

species i.e. skin color that too during migration. It is actually a representation of a finite amount of area at surface of the aquatic species. The analogy that could be used here is a comparison of rigid body to a particle. We are only interested in the effects of the skin color to the skin friction drag at any given point of the specimen; the surface temperature for one given area is treated no different than another. Thus, an area at the midpoint of a fish that moves very slightly during fish's motion, compared to the tip of the tail or nose of the specimen are equal in terms of surface properties on a finite level.

Various tests are carried out inside and outside of the water on black and white color plates. Black plates with different materials (aluminum, carbon sheet, and plastic) are also tested inside and outside the water. In Fig. 6(a) and (b), the surface temperature of the black plates with different materials inside and outside of the water are shown, respectively. As demonstrated in Fig. 6, once the plates are outside the water, the surface temperatures are higher compared to plates inside. Moreover, it can be concluded that depending on the type of the material, the surface temperature is also changing. Fig. 6(a) shows that the plastic plate has higher temperatures once the plate is outside of the water, followed by a carbon sheet and aluminum plate, respectively. However, this trend changes once the plates are inside. It is visible from Fig. 6(b) that for radiation less than 715 W/m$^2$ (time: 6 min) the black carbon sheet has the highest surface temperature followed by aluminum and plastic plates. This trend will be different for higher radiations so that the plastic plate shows higher values of surface temperature compared to aluminum and carbon plates. This can be explained by the difference of conductivity of different materials inside the water.

In Fig. 7(a) and (b), the surface temperature of the aluminum black plate inside and outside of the water and the comparison for black and white colors are shown, respectively.

As can be seen in Fig. 7(a), the surface temperature of the plate with black color is decreasing by almost 10%, once the water covers the top surface of the plate. Moreover, it can be found from Fig. 7(b) that the black plate floating over the water has a higher surface temperature than the white plate. To investigate the effects of water on the surface temperature of the flat plates, the same study is carried out for black and white plates on a wood-base. In Fig. 8(a), (b), (c), and (d) the surface temperatures for the carbon and plastic black plates, and black and white aluminum plates on a wood-base are indicated, respectively. A thermal camera and laser thermometer are used to measure the

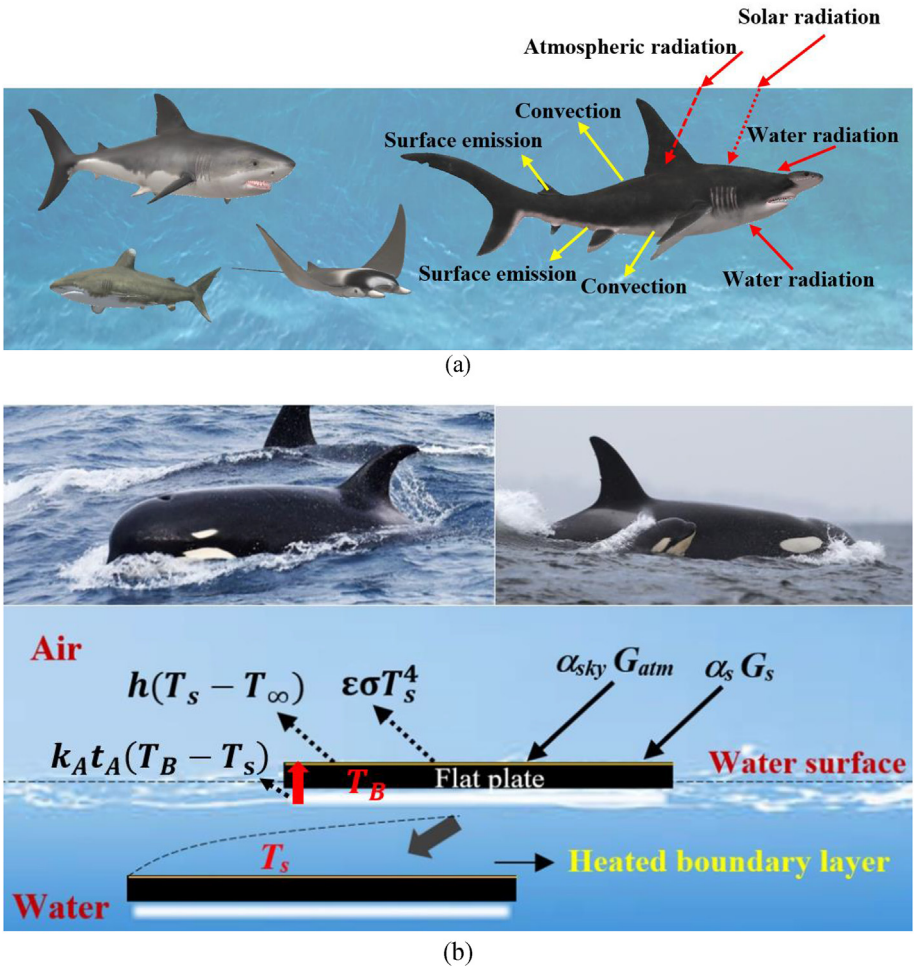


**Fig. 12.** (a) heat fluxes on aquatics' body and (b) energy balance for a flat plate outside the water.

**Table 2**
Values for the parameters of energy balance (Hassanalian et al., 2018a) (Hassanalian et al., 2018b) (Kvadsheim et al., 1996).

| Parameter | Value |
|---|---|
| Solar absorptivity of surface ($\alpha_s$) | Dark black (0.97), light white (0.21) |
| Solar absorptivity of sky ($\alpha_{sky}$) | ≈0.8 |
| Emissivity of surface ($\varepsilon$) | 0.8 |
| Stefan–Boltzmann constant ($\sigma$) | $5.67036 \times 10^{-8}$ W/m$^2$K$^4$ |
| Ambient temperature ($T_a$) | 16.1 °C |
| Air pressure coefficient ($c_p$) | 1000 |
| Conductivity of the blubber ($k_A$) | 0.2 W/mK |
| Blubber thickness for Killer whales and dolphins ($t_A$) | 0.3 m |

surface temperatures of each plate. Using these two techniques to gather the same results confirmed the temperature measurement's accuracy.

Fig. 9(a) and (b) demonstrate the comparison of surface temperature for the wood-base black and white aluminum plates and black plates from aluminum, carbon, and plastic, respectively. It is evident from Fig. 9(a) that a maximum temperature difference of 22 °C can be found between black and white colored aluminum plates. Fig. 9(b) exhibits higher values of surface temperature for plastic plate than carbon and aluminum plates. These high values of difference can be explained by the type of the materials and their conductivity. Between these three materials the aluminum black plate has the lowest surface temperatures due to its higher value of conductivity.

In Fig. 10(a)–(c), the surface temperature distributions are shown for black and white aluminum flat plates and for white and black plates from aluminum, carbon, and plastic, respectively. It is investigated by a thermal camera, so that for a similar value of the radiation, different surface temperatures can be recorded for black and white color plates.

In Fig. 11(a)–(c), the comparison of surface temperature for the carbon, aluminum, and plastic black plates with two different bases (wood and water) are shown, respectively. The results show that there is a temperature difference depending on the base of the experiment. This difference shows the conductivity and convection effects of the environment on surface temperature. It is clear that for water-base experiment the surface temperatures of the black color plates exposed to the same radiations decrease drastically compared to the wood-base experiment. At the highest value of the radiation, the black plastic plate has the highest surface temperature in water and wood-base cases, followed by carbon and aluminum plates.

It should be emphasized that during migrations, Dusky dolphins are barely submerged or even slightly breaching the water as they tend to play because they are social creatures and interact with each other. The tendency of remaining at or closer to water surface holds true for Orcas/Killer Whales as well during their laborious and extensive motion. The current work focuses on the marvel the evolution is. It has given the animals, characteristics that support their prolonged motions during hectic migration. Therefore, focus has been analyses at surface. Furthermore, if color effects on general swimming tendencies (deep water) of Dusky dolphins and Orcas/Killer whales are to be studied, it would indeed require a different experimentation setup than the one utilized above since the focus would not be at or near surface. Similar precaution of experiment for fish such as billfish, which swim deep and

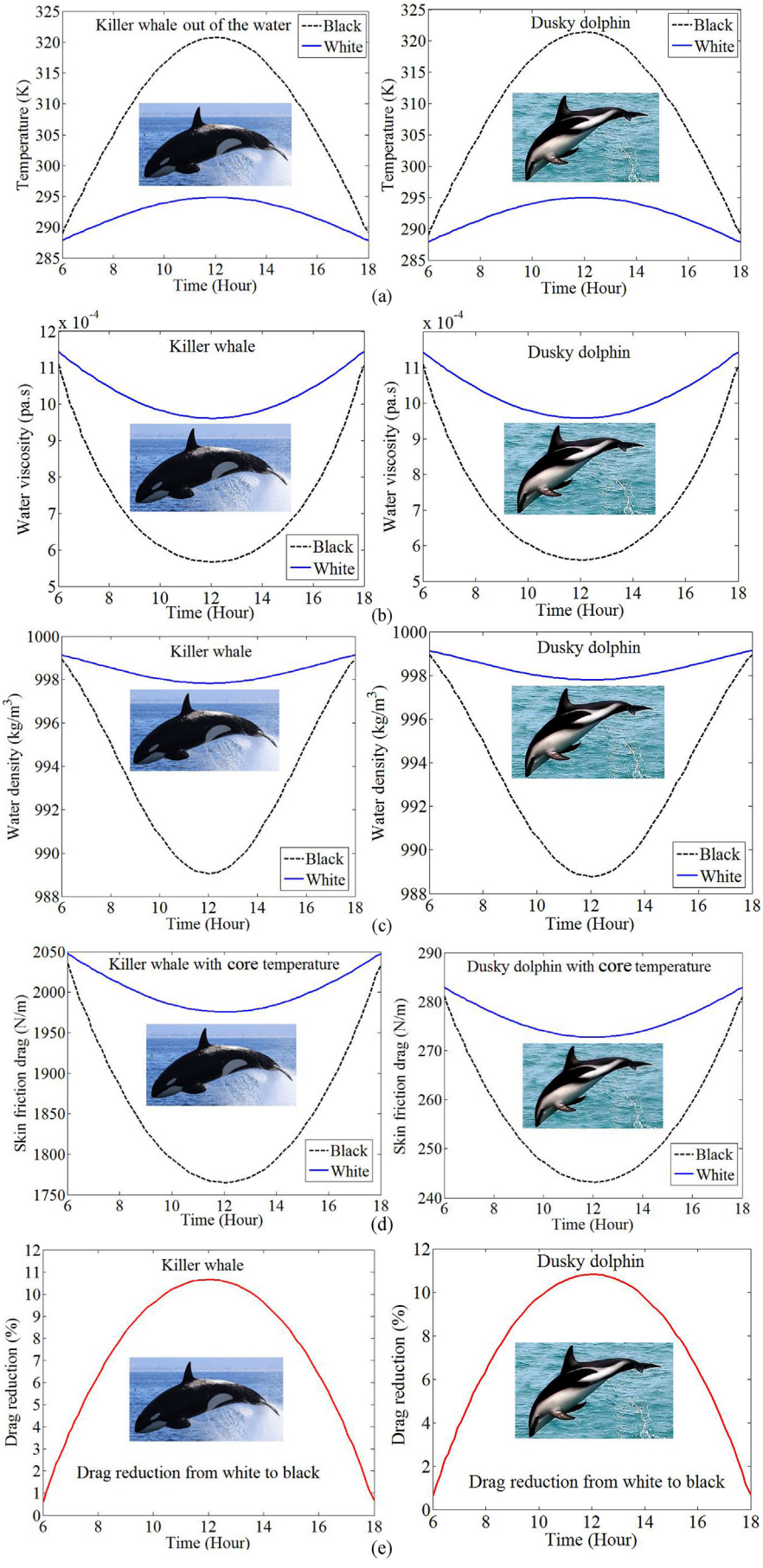


*(caption on next page)*

**Fig. 13.** Diagrams of (a) surface temperature, (b) water viscosity, (c) water density, (d) skin friction drag, and (e) drag reduction percentage versus time for Killer whales and Dusky dolphins.

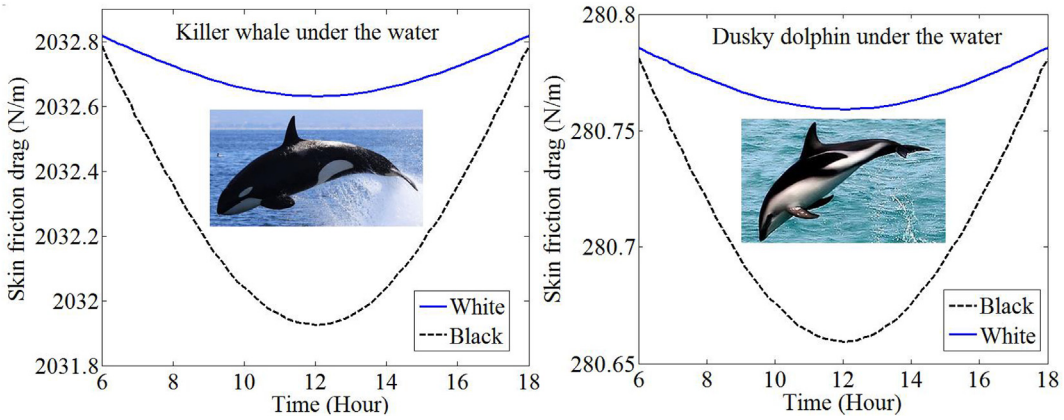


**Fig. 14.** Skin friction drag versus time for Killer whales and Dusky dolphins in water.

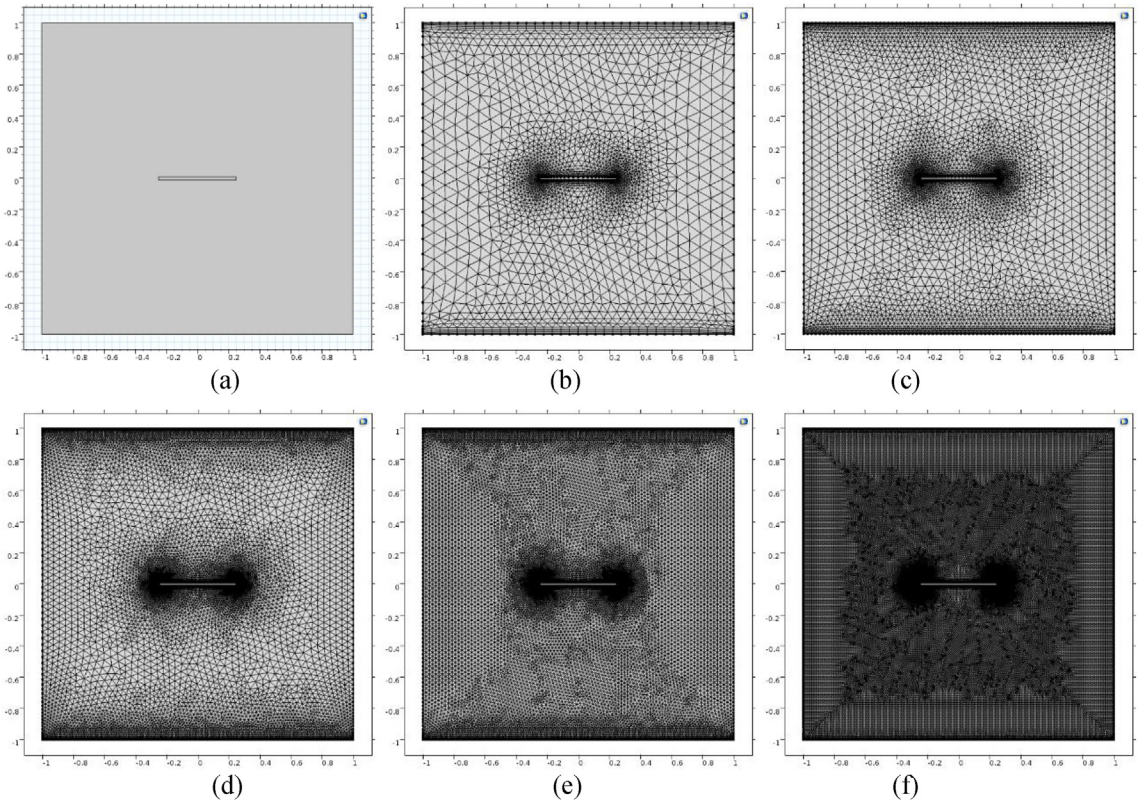


**Fig. 15.** Views of (a) case study, (b) normal, (c) fine, (d) finer, (e) extra fine, and (f) extremely fine meshes.

where the amount of light penetration may significantly change, should be taken.

It is important to mention here that the tissue structure by itself does have an impact on the surface temperature of the animal. This fact is indeed elaborated in Figs. 6(a), 8(a)-8(c) and 9(b) where three different materials of same color have been considered namely plastic, carbon and aluminum. Over the entire length of time, plastic exhibits the most temperature at every time followed by carbon and aluminum. Between these three materials the aluminum plate has the lowest surface temperatures due to its higher value of conductivity. These results point to the important aspect of this whole surface-temperature-conundrum that tissue or material structure cannot be overlooked. Having said that, color effects have their own contribution. A separate analysis have been performed above depicted in different plots. Fig. 7(b) shows that black plate outside water (partially submerged) has more temperature than its white counterpart for nearly the entire length of temperature variation and time. Same results are also exhibited by Figs. 8(c), (d) and 9(a) that also has an Aluminum plate with a wooden base. Therefore, the present work cannot encompass the percentage impact of tissue structure and color on surface temperature.

A detailed analysis that would include different animal tissues with same color, and same tissue with different colors would be needed that goes well beyond the scope as well as the purpose of the current work. The present work takes the reader as well as the scientific community one step closer to making efficient Unmanned Underwater Vehicles (UUVs) and amphibian drones. The importance of black color trend

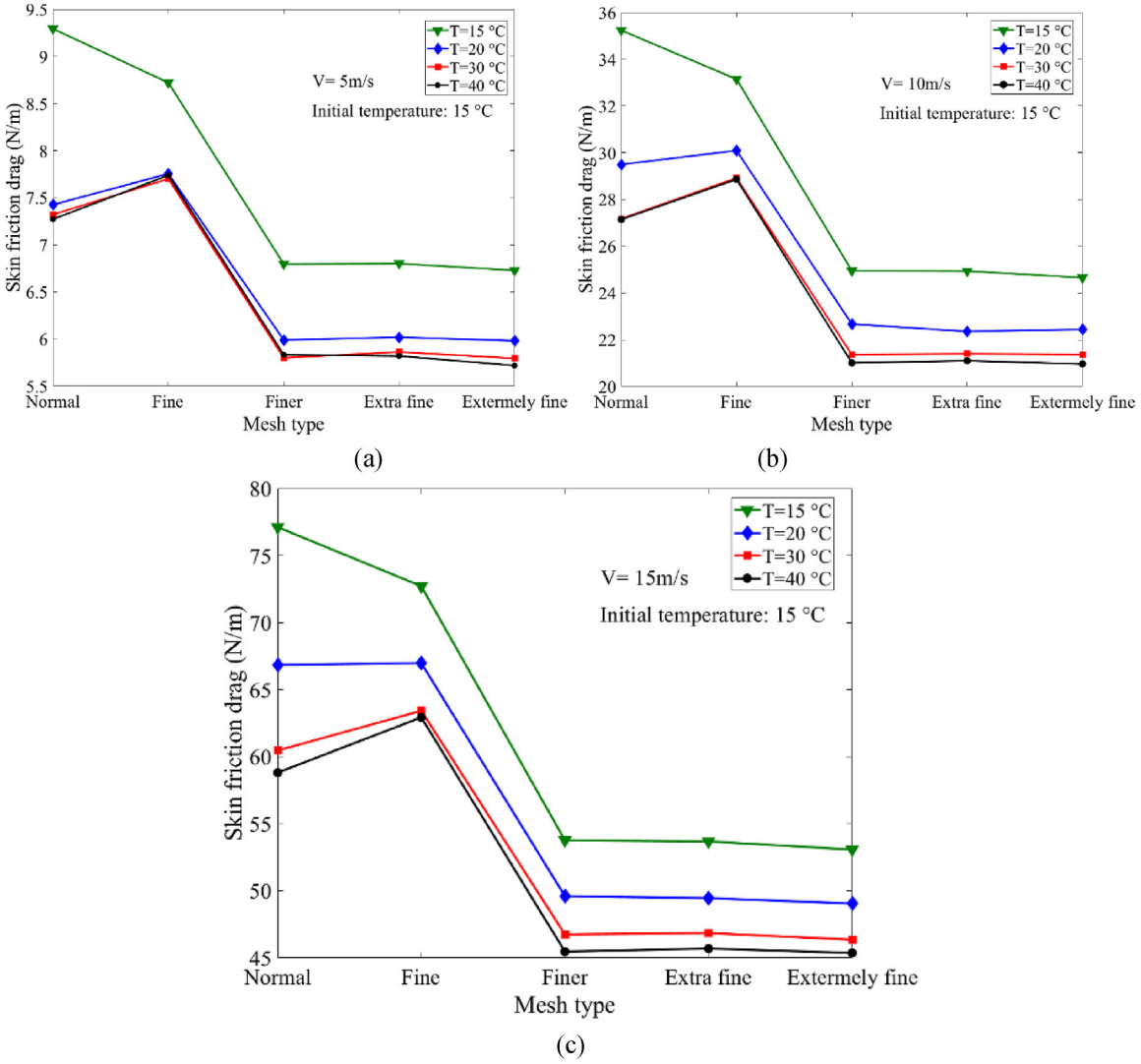


**Fig. 16.** Views of skin friction drag for different mesh types and surface temperature in flow speed of (a) 5 m/s, (b) 10 m/s, and (c) 15 m/s.

presented in the mathematical predictions as well as experimental results presented here can be put to the test on real engineering system of UUV or amphibian drone. The actual material used on the engineering system would be tested for black and then white colors to have real trends. Both the tasks of impact of tissue structure of an animal on surface temperature and actual benefit of color on UUV and amphibious drones are separate future work that are interesting and have immense utility.

## 5. Modeling, energy balance, and governing equations

In this study, aquatics like Killer whales and Dusky dolphins as the fastest marine organisms with a dark color on the top and white color at the bottom side of their bodies are considered. The temperature near the boundary layer can be modeled using the heat transfer phenomena. The top of the body is exposed to solar, atmospheric and water radiation and the bottom part is exposed to water radiation. The conduction of heat between the top and the bottom sides is neglected in this modeling. Heat exchange with the water will be due to convection and radiation, in the top and bottom sides of the considered aquatics' bodies. For simplicity, the bottom side is considered adiabatic. In other words, in this study, only the top side is considered for thermal-fluid analysis.

As can be seen in the oceanic wildlife, sometimes the bodies of some of the aquatics like Killer whales and Dusky dolphins with black color on top is outside the water. As indicated in Fig. 12, the incoming energy from the solar, atmospheric and water radiations for the top part, and the ocean radiations for the bottom part of the aquatic's body can be balanced by convection to the freestream and radiative surface emission. It should be noted that fishes are usually considered cold-blooded animals, thus their skin temperatures should be the same as the surrounding water. Some other aquatics like Killer whale and Dusky dolphin are warm-blooded, such that their core and skin temperatures are higher than the surrounding water. Moreover, the intensity will decrease due to water dissipation and this factor will be included in the modeling.

It is important to note here that in all the equations that would be used from here onwards in the mathematical modeling, the effect of the motion of the dolphin is incorporated as in Fluid Mechanics. This effect of motion of a body in a low velocity fluid is equivalent to a stationary body surrounded with moving flow (Graebel, 2007). The speed of water current in the ocean is usually very negligible comparing to the speed of the dolphin (order of 2.5 m/s) (Kelly et al., 2001). The main objective behind the modeling is to put into consideration the effect of the color to have them corroborate with the performed experiments.

A general energy balance equation can be written for the top side of the aquatics, as follows:

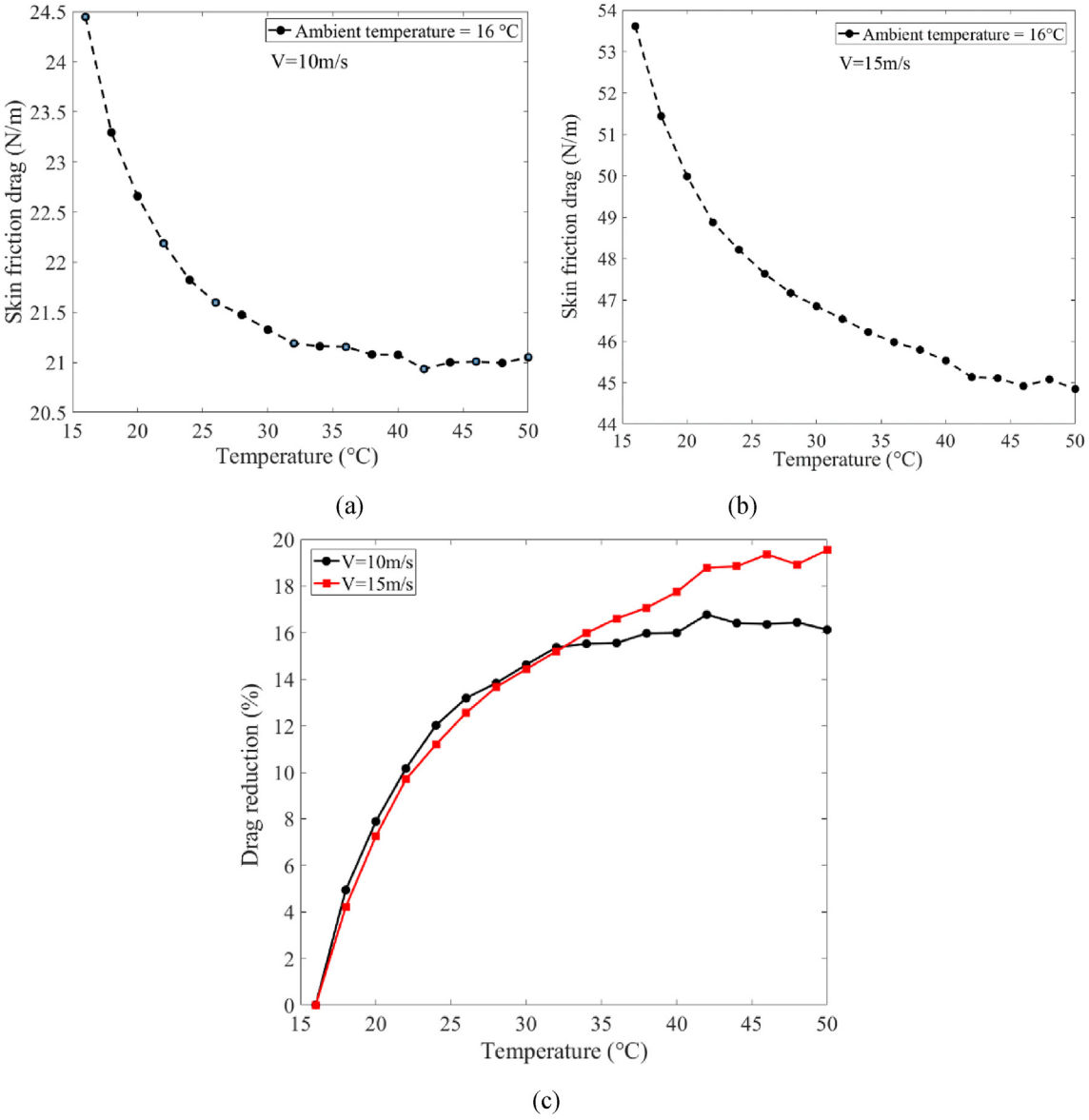


**Fig. 17.** Views of skin friction drag versus temperature for a flow speed of (a) 10 m/s, (b) 15 m/s, and (c) drag reduction percentage versus surface temperature.

$$\zeta(\alpha_s G_s + \alpha_{sky} G_{atm}) + \alpha_w G_w + k_A t_A (T_B - T_{S_u}) = h(T_{S_u} - T_\infty) + \varepsilon\sigma T_{S_u}^4 \quad (2)$$

where $\alpha_s$, $\alpha_w$, $\alpha_{sky}$, $\varepsilon$, $\zeta$, $\sigma$, $k_A$, $t_A$, $G_s$, $G_{atm}$, $G_w$, $h$, $T_B$, $T_{Su}$, $T_{Sl}$, and $T_\infty$ are the solar absorptivity of surface, absorptivity of water, absorptivity of sky, emissivity of surface, light penetration factor, Stefan–Boltzmann constant, conductivity of the blubber, blubber thickness, solar radiation, radiation at the Earth's surface due to atmospheric emission, water radiation, convective heat transfer coefficient, core temperature of aquatic, upper and lower surface temperatures, and background environment temperature, respectively. As can be shown from geometric and physical characteristics of the mentioned aquatics in Table 1, all the case studies are in the turbulent regime of the flow.

To compare the effects of the colors, a flat plate is considered in the rest of this work. In this case study, a flat plate with a core temperature is analyzed. It is assumed that a flat plate is moving over the surface of the water and receiving heat from the sun and atmosphere radiations, in order to increase its surface temperature. Then, the heated plate will continue moving under the water. The energy balance for this case with a core temperature is modeled as follows:

$$\alpha_s G_s + \alpha_{sky} G_{atm} + k_A t_A (T_B - T_{S_u}) = h(T_{S_u} - T_\infty) + \varepsilon\sigma T_{S_u}^4 \quad (3)$$

As the flat plate is moving over the water, the convection is happening between the air and flat plate. The convective heat transfer coefficient for turbulent flow is calculated as (Bergman et al., 2007):

$$Nu = 0.037 Re_L^{\frac{4}{5}} Pr^{\frac{1}{3}} \quad (4)$$

where $Nu$, $Re$, and $P_r$ represent Nusselt number, Reynolds number, and Prandtl number. The Reynolds number is expressed as:

$$Re = \frac{\rho_a c V}{\mu} \quad (5)$$

where $\rho_a$ and $\mu$ are the ambient air density and dynamic viscosity coefficient respectively, $c$ is the body cord length, and $V$ is the swimming speed of the considered aquatic. Substituting the values of $Re$ and $Pr$ in Eq. (4), $Nu$ is obtained. $Nu$ can be also expressed as (Bergman et al., 2007):

$$Nu = \frac{hc}{k_f} \rightarrow h = Nu\frac{k_f}{c_p} \quad (6)$$

where $k_f$ is the thermal conductivity of the air. By substituting the

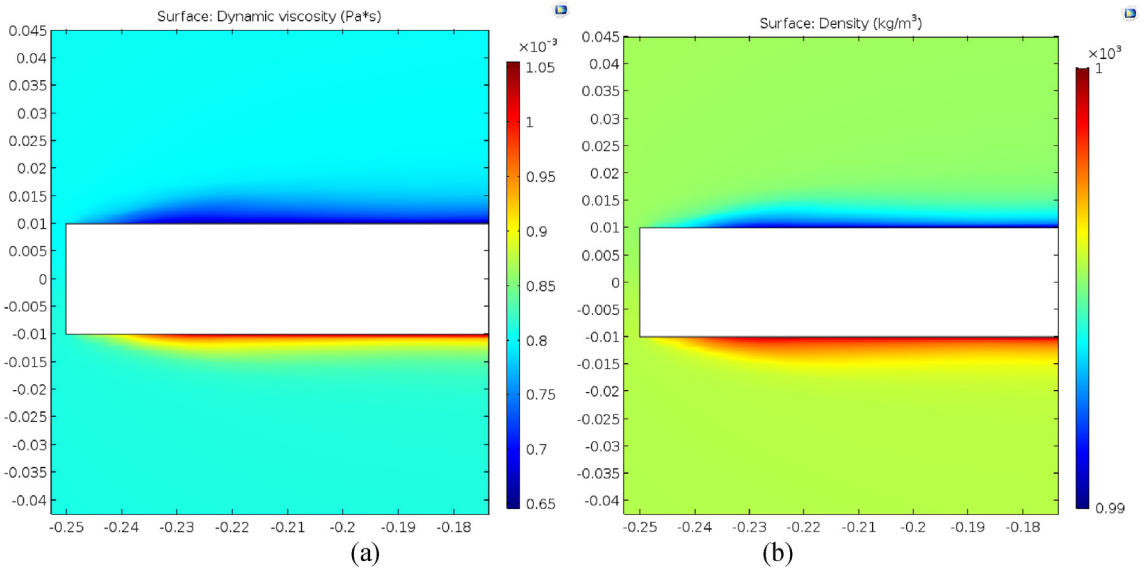


**Fig. 18.** Views of (a) dynamic viscosity and (b) density of the flat plate with an upper temperature of 42 °C and flow speed of 15 m/s.

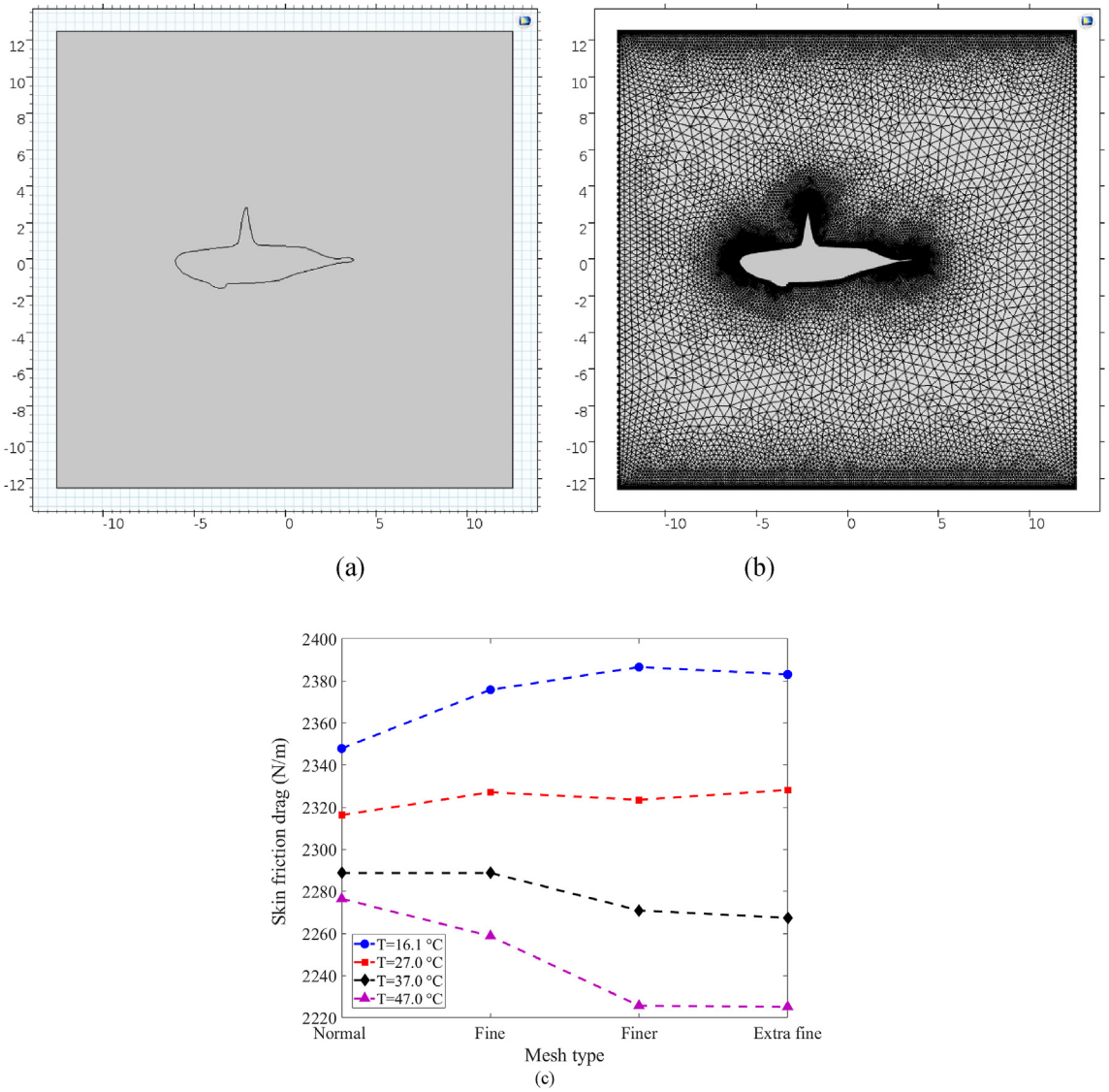


**Fig. 19.** Views of (a) case study, (b) 'finer' mesh, and (c) skin friction drag for different mesh types and surface temperature in flow speed of 15.6 m/s.

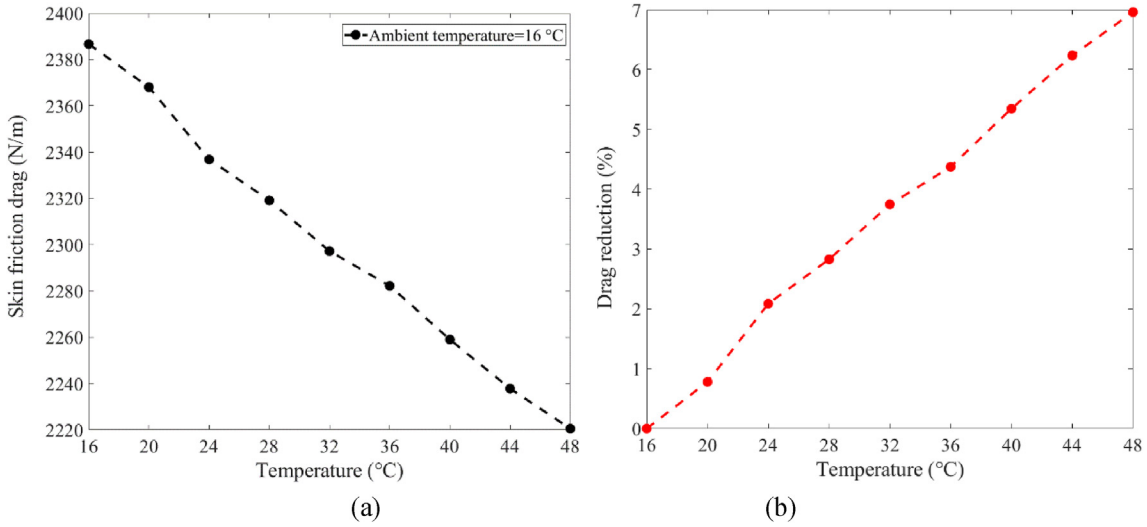


**Fig. 20.** Views of (a) skin friction drag versus temperature for a Killer whale and (b) drag reduction percentage versus surface temperature.

values of $Nu$, $k_f$ and $c$, the convective heat transfer coefficient is calculated. Solving Eq. (3), the surface temperature of the upper sides of the aquatic's body can be calculated. Then, the obtained surface temperatures are used to derive the dynamic viscosity and density of the water around the aquatics, after diving into the water. In Table 2, the values for the parameters of energy balance are shown.

## 6. Turbulent flow and skin friction drag calculation

To study the effect of the surface temperature on swimming performance of the Killer whales and Dusky dolphins, the skin friction drag for the top part of their bodies is evaluated. In this study, the curvature of the body of these aquatics is ignored, and the boundary layer on a flat plate is assumed. Since the flow regime over each face of these aquatics is turbulent, the 1/5 power law boundary layer for turbulent flow is considered. The effects of the thermal boundary layer on the skin friction forces for top sides are calculated for tropical regions. Finally, the drag force ($D$) over the top side can be expressed as follows (Bushnell and Hefner, 1990):

$$D' = 0.03625\rho V^2 L Re_L^{-\frac{1}{5}} \tag{7}$$

where $D'$, $L$, $Re_L$ are drag per unit width, length of aquatic's body, and Reynolds number, respectively.

To understand the effects of the calculated surface temperatures on shear stress, the viscosity and density are expressed as function of temperature. For dynamic viscosity variation (mPa.s), the Vogel method is applied and shown below (Mehrotra et al., 1996).

$$\mu = e^{A+\frac{B}{C+T}} \tag{8}$$

where $A$, $B$, and $C$ are constants, which for water are equal to $-3.7188$, 578.919, and $-137.546$, respectively, and $T$ is temperature (K). The density for air-free water is also modeled as (Jones and Harris, 1992):

$$\rho = 999.85308 + 6.32693 \times 10^{-2}T - 8.523829 \times 10^{-3}T^2 + 6.943248 \times 10^{-5}T^3 - 3.821216 \times 10^{-7}T^4 \tag{9}$$

where $T$ represents the reference water temperature (°C).

Implementing the extracted values for solar radiation of the tropical regions and the characteristics of the Killer whales and Dusky dolphins, the changes in temperature, density and viscosity of boundary layer over the body and upper skin drag, are calculated for two considered aquatics with black and white colors. In Fig. 13(a)–(e), the changes of surface temperatures, water density, water viscosity, skin friction drag, and drag reduction percentages for Killer whales and Dusky dolphins are shown, respectively.

Considering the location of tropical regions as an example for the Killer whales and Dusky dolphins, the hourly variations of their skin temperatures are calculated. As shown in Fig. 13(a), at midday the surface temperature of these aquatics with black color on the top reaches to 320 K which is almost 25 °C warmer compared to the white color. This modeling also verifies the performed experimental study on the effects of color on surface temperature. Moreover, the Fig. 13(b) and (c) demonstrate that the density and viscosity of the water in the boundary layer of these aquatics decrease with increase in the surface temperatures which consequently decrease the skin friction drag as shown in Fig. 13(d). In Fig. 13(e), the percentage of the drag reduction is indicated for the Killer whales and Dusky dolphins and it can be seen at midday that the skin drag when the top part of the body is black can reduce to 11%, compared to the white color.

Considering the total body of Killer whales and Dusky dolphins inside the water, the same modeling can be carried out on these aquatics. Solving the energy balance in Eq. (2), the skin friction drag of Killer whales and Dusky dolphins are obtained as shown in Fig. 14. The results indicate that there is a negligible color effect once these aquatics are under the water.

## 7. Computational modeling of a flat plate underwater

To study the effects of the surface temperature in turbulent flow on skin friction drag, COMSOL Multiphysics is used for analysis. A simple flat plate with a length of 50 cm and thickness of 2 cm inside the fluid domain of 2 m by 2 m is considered as a 2D model for this study as shown in Fig. 15(a). Fluid and solid domains are chosen to be water and meat, respectively. Fluid flow is considered to be turbulent and $k$-$\varepsilon$ method is applied. Among many different formulations for solving turbulent flow, $k$-$\varepsilon$ is used in this study because of its fast convergence and low computational cost. In addition, it performs well for flows around an object which is the case in this study. As indicated in Fig. 15(b)–(f), five different kinds of mesh including normal, fine, finer, extra fine and extremely fine are used to study the mesh independence of the analyses to make sure that the results are independent of mesh type.

For this study, the skin drag is calculated for the top surface of the flat plate with different temperatures (15, 20, 30 and 40 °C) at speeds of 5, 10, and 15 m/s. It is clear from Fig. 16 that after 'Finer' mesh type, the results do not change significantly. Therefore, in order to optimize the computational costs 'Finer' mesh is used to obtain results.

To study the effects of the surface temperature and the flow speed

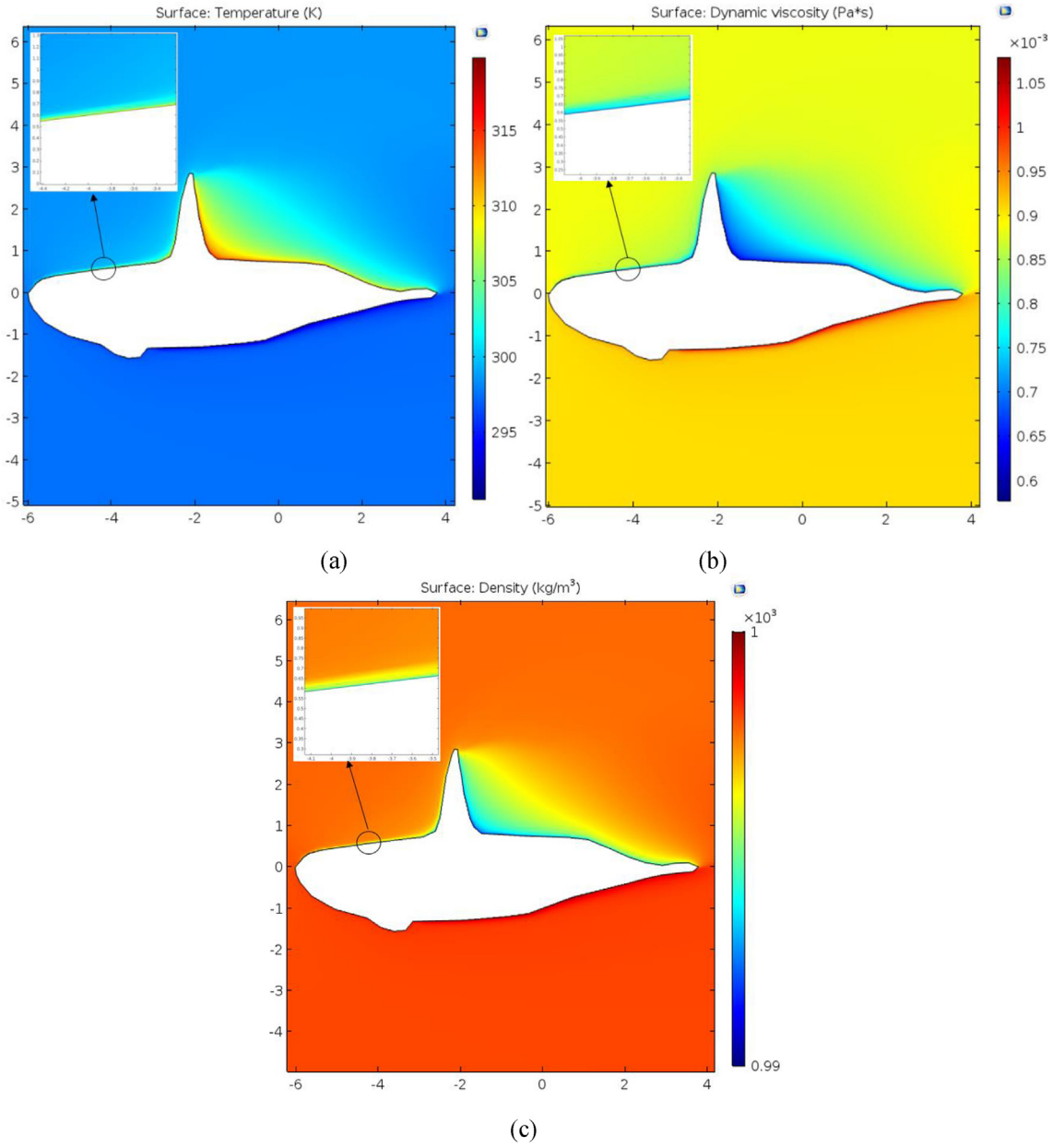


**Fig. 21.** Views of (a) temperature, (b) dynamic viscosity, and (c) density around the Killer whale with an upper temperature of 48 °C and flow speed of 15.6 m/s.

on the skin friction drag of the modeled flat plate, different analyses are carried out in COMSOL. In Fig. 17(a) and (b), the skin friction drag and in Fig. 17(a) the percentage of drag reduction for flow speeds of 10 m/s and 15 m/s in different temperatures are shown. The results in Fig. 17(a) and (b) indicates that the skin friction drags for temperatures higher than 40 °C are changing slightly with increasing the surface temperature. As can be seen in Fig. 17(c), for temperatures less than 34 °C, the lower speed flow (10 m/s) has more drag reduction, but after that with increasing the surface temperature, the drag reduction for higher speed flow (15 m/s) increases drastically. It should be noted that the reference skin friction drag for shown percentages in Fig. 17(c) is calculated in an ambient temperature of 16 °C.

As can be seen from Fig. 18(a) and (b), dynamic viscosity and the density of the fluid are highly related to the surface temperature. With an increase of plate surface temperature, viscosity decreases which can be seen in Fig. 18(a). In the vicinity of the plate's top surface with higher surface temperature compared to bottom surface and fluid itself, dynamic viscosity is significantly lower than the bottom surface. Similarly, this can be asserted about density; the density of the fluid in the upper surface is less than the lower surface. Skin drag force also depends on density and viscosity, thus drag force is affected by temperature difference.

## 8. Computational modeling of a killer whale underwater

COMSOL Multiphysics is applied to measure the skin friction drag around a 2D model of Killer whale. The modeled Killer whale as shown in Fig. 19(a) has a length of 9.8 m inside the fluid domain of 25 m by 25 m. The applied analysis for flat plate is also used for Killer whale. Four different kinds of mesh including normal, fine, finer, and extra fine are used to study the convergence of the analysis. Fig. 19(c) indicates that after 'finer' mesh, the results are almost similar. Therefore, 'finer' mesh is selected for the rest of analysis. In Fig. 19(b), the applied 'finer' mesh for thermal-fluid analysis around a Killer whale is shown.

In Fig. 20(a) and (b), the skin friction drag around a Killer whale for different surface temperatures and the percentage of drag reduction for

flow speed of 15.6 m/s are shown, respectively. The results in Fig. 20(a) demonstrate a linear drag reduction with increasing the top surface temperature of the Killer whale. A maximum skin drag reduction of 7% can be achieved in a top surface temperature of 48 °C, as indicated in Fig. 20(b).

It is visible from Fig. 21(a) that the fluid at the top side of the Killer whale has a higher temperature than the bottom side. As demonstrated in Fig. 21(b) and (c), similar to a flat plate, the Killer whale also has dynamic viscosity and the density of the fluid at the top of its body decrease, owing to an increase in the top surface temperature. In other words, in the vicinity of the top surface of Killer whale with higher surface temperature compared to the bottom surface and fluid itself, dynamic viscosity and the density are significantly lower than the bottom surface. A decrease in viscosity and density of flow around the Killer whale consequently decrease the skin friction drag force.

## 9. Conclusions

Thermal analysis was carried-out in aquatic animals like Killer whales and Dusky dolphins which swim in various bodies of water and possess a combination of black and white color. The surrounding fluxes, such as the sky and sun radiation as well as the core temperatures were considered in an energy balance to determine the skin surface temperatures of considered organisms' bodies. Experimental studies were performed on a black and white aluminum, black carbon, and black plastic flat plates to study the effects of their emissivity on their surface temperature. It was shown that black color is heated more than white color in the same condition. Moreover, a 1/5 power law boundary layer for a turbulent flow was used to determine an analytical expression for the skin drag of Killer whales and Dusky dolphins. It was indicated that, at midday, there is a drag reduction of 11% for the black top than the white top color in these aquatics. A computational study was also performed in COMSOL to investigate the effects of the surface temperature of a flat plate and a 2D modeled Killer whales underwater. The results showed that Killer whales can achieve a drag reduction of 7% in a surface temperature of 48 °C.

## References


Adelard, L., Pignolet-Tardan, F., Mara, T., Lauret, P., Garde, F., Boyer, H., 1998. Sky temperature modelisation and applications in building simulation. Renew. Energy 15 (1), 418–430.

Ahlborn, B.K., Blake, R.W., Chan, K.H., 2009. Optimal fineness ratio for minimum drag in large whales. Can. J. Zool. 87 (2), 124–131.

American Cetacean Society, 2013. Daily Zooniverse. Retrieved from. https://daily.zooniverse.org/2013/11/02/theyre-everywhere/.

American Cetacean Society, 2017. acsonline. Retrieved from. https://www.acsonline.org/bottlenose-dolphin?.

Baird, R.W., Baird, R.W., 2006. Killer Whales of the World: Natural History and Conservation. MBI Publishing Company LLC.

Bergman, T.L., Incropera, F.P., DeWitt, D.P., Lavine, A.S., 2007. Fundamentals of Heat and Mass Transfer, seventh ed. John Wiley & Sons.

Bushnell, D.M., Hefner, J.N. (Eds.), 1990. Viscous Drag Reduction in Boundary Layers. American Institute of Aeronautics and Astronautics.

Bushnell, D.M., Moore, K.J., 1991. Drag reduction in nature. Annu. Rev. Fluid Mech. 23 (1), 65–79.

Cho, S.H., Tae, C.S., Zaheeruddin, M., 2007. Effect of fluid velocity, temperature, and concentration of non-ionic surfactants on drag reduction. Energy Convers. Manag. 48 (3), 913–918.

Dahlheim, M.E., Heyning, J.E., 1999. In: Killer Whale Orcinus orca (Linnaeus, 1758), vol. 6 Handbook of marine mammals.

Deakos, M.H., 2010. Ecology and Social Behavior of a Resident Manta Ray( Manta Alfredi) Population off Maui, Hawai'i. Dissertation. University of Hawai'i at Mānoa.

Dewar, H., Mous, P., Domeier, M., Muljadi, A., Pet, J., Whitty, J., 2008. Movements and site fidelity of the giant manta ray, Manta birostris, in the Komodo Marine Park, Indonesia. Mar. Biol. 155 (2), 121–133.

Ebert, D., 2003. Sharks, Rays, and Chimaeras of California. Univ of California Press, Berkeley.

Ehrhardt, N.M., Fitchett, M.D., 2006. On the seasonal dynamic characteristics of the sailfish, Istiophorus platypterus, in the eastern Pacific off Central America. Bull. Mar. Sci. 79 (3), 589–606.

Fish, F.E., 2006. The myth and reality of Gray's paradox: implication of dolphin drag reduction for technology. Bioinspiration Biomimetics 1 (2), 17–25.

Fish, F.E., 2013. Advantages of natural propulsive systems. Mar. Technol. Soc. J. 47 (5), 37–44.

Fish, F., Schreiber, C., Moored, K., Liu, G., Dong, H., Bart-Smith, H., 2016. Hydrodynamic performance of aquatic flapping: efficiency of underwater flight in the manta. Aerospace 3 (3), 25.

Ford, J.K., 2009. Killer whale: Orcinus orca. In: Encyclopedia of Marine Mammals. Academic Press, Elsevier.

Fritsches, K.A., Brill, R.W., Warrant, E.J., 2005. Warm eyes provide superior vision in swordfishes. Curr. Biol. 15 (1), 55–58.

Gardieff, S., 2017. Discover Fishes. Retrieved from Florida Museum of Natural History: https://www.floridamuseum.ufl.edu/discover-fish/species-profiles/istiophorus-platypterus/.

Gibson, A., 2002. Sharks. St. Martin's Press, Nature, New York.

Graebel, W., 2007. Advanced Fluid Mechanics. Academic Press.

Handara, V.A., Illya, G., Tippabhotla, S.K., Shivakumar, R., Budiman, A.S., 2016. Center for solar photovoltaics (CPV) at surya university: novel and innovative solar photovoltaics system designs for tropical and near-ocean regions (an overview and research directions). ProcediaEngineering 139, 22–31.

Hassanalian, M., Abdelkefi, A., Wei, M., Ziaei-Rad, S., 2017a. A novel methodology for wing sizing of bio-inspired flapping wing micro air vehicles: theory and prototype. Acta Mech. 228 (3), 1097–1113.

Hassanalian, M., Abdelmoula, H., Ayed, S.B., Abdelkefi, A., 2017b. Thermal impact of migrating birds' wing color on their flight performance: possibility of new generation of biologically inspired drones. J. Therm. Biol. 66, 27–32.

Hassanalian, M., Ayed, S.B., Ali, M., Houde, P., Hocut, C., Abdelkefi, A., 2018a. Insights on the thermal impacts of wing colorization of migrating birds on their skin friction drag and the choice of their flight route. J. Therm. Biol. 72, 81–93.

Hassanalian, M., Throneberry, G., Ali, M., Ayed, S.B., Abdelkefi, A., 2018b. Role of wing color and seasonal changes in ambient temperature and solar irradiation on predicted flight efficiency of the Albatross. J. Therm. Biol. 71, 112–122.

Hastie, G.D., Swift, R.J., Slesser, G., Thompson, P.M., Turrell, W.R., 2005. Environmental models for predicting oceanic dolphin habitat in the Northeast Atlantic. ICES J. Mar. Sci. 62 (4), 760–770.

Helfman, G., Collette, B.B., Facey, D.E., Bowen, B.W., 2009. The Diversity of Fishes: Biology, Evolution, and Ecology. John Wiley & Sons.

Hoyt, J.W., 1975. Hydrodynamic drag reduction due to fish slimes. In: Swimming and Flying in Nature. Springer, Boston, MA.

Jones, F.E., Harris, G.L., 1992. ITS-90 density of water formulation for volumetric standards calibration. Journal of research of the National Institute of Standards and Technology 97 (3), 335.

Kasting, N.W., Adderley, S.A., Safford, T., Hewlett, K.G., 1989. Thermoregulation in beluga (Delphinapterus leucas) and killer (Orcinus orca) whales. Physiol. Zool. 62 (3), 687–701.

Kerstetter, D.W., Bayse, S.M., Fenton, J.L., Graves, J.E., 2011. Sailfish habitat utilization and vertical movements in the southern Gulf of Mexico and Florida Straits. Marine and Coastal Fisheries 3 (1), 353–365.

Kelly, K.A., Dickinson, S., McPhaden, M.J., Johnson, G.C., 2001. Ocean currents evident in satellite wind data. Geophys. Res. Lett. 28 (12), 2469–2472.

Klimley, A.P., 2013. The Biology of Sharks and Rays. University of Chicago Press.

Kvadsheim, P.H., Folkow, L.P., Blix, A.S., 1996. Thermal conductivity of minke whale blubber. J. Therm. Biol. 21 (2), 123–128.

Lam, C.H., Galuardi, B., Mendillo, A., Chandler, E., Lutcavage, M.E., 2016. Sailfish migrations connect productive coastal areas in the West Atlantic Ocean. Sci. Rep. 6, 38163.

Last, P., Naylor, G., Séret, B., White, W., de Carvalho, M., Stehmann, M. (Eds.), 2016. Rays of the World. Cornell University Press.

Li, F.C., Kawaguchi, Y., Hishida, K., 2004. Investigation on the characteristics of turbulence transport for momentum and heat in a drag-reducing surfactant solution flow. Phys. Fluids 16 (9), 3281–3295.

Lu, C.P., Bremer, J.R.A., McKenzie, J.L., Chiang, W.C., 2015. Analysis of sailfish (istiophorus platypterus) population structure in the North Pacific Ocean. Fish. Res. 166, 33–38.

Macdonald, D.W., 1995. The Encyclopedia of Mammals. Checkmark Books, New York.

Mann, J., Connor, R.C., Tyack, P.L., Whitehead, H. (Eds.), 2000. Cetacean Societies: Field Studies of Dolphins and Whales. University of Chicago Press.

Marras, S., Noda, T., Steffensen, J.F., Svendsen, M.B., Krause, J., Wilson, A.D., Kurvers, R.H., Herbert-Read, J., Boswell, K.M., Domenici, P., 2015. Not so fast: swimming behavior of sailfish during predator–prey interactions using high-speed video and accelerometry. Integr. Comp. Biol. 55 (4), 719–727.

Marshall, A.D., Compagno, L.J., Bennett, M.B., 2009. Redescription of the genus manta with resurrection of manta alfredi (krefft, 1868)(chondrichthyes; myliobatoidei; mobulidae). Zootaxa 2301, 1–28.

Martin, S., Bhushan, B., 2014. Fluid flow analysis of a shark-inspired microstructure. J. Fluid Mech. 756, 5–29.

Mehrotra, A.K., Monnery, W.D., Svrcek, W.Y., 1996. A review of practical calculation methods for the viscosity of liquid hydrocarbons and their mixtures. Fluid Phase Equilib. 117 (1–2), 344–355.

Mirzaeinia, A., Hassanalian, M., Lee, K., Mirzaeinia, M., 2019. Performance Enhancement and Load Balancing of Swarming Drones through Position Reconfiguration. 2019 AIAA Aviation Forum, Dallas, TX.

Murchison, A.E., Magnuson, J.J., 1966. Notes on the Coloration and Behavior of the Common Dolphin. Coryphaena hippurus.

Peeters, J.W., Pecnik, R., Rohde, M., Van Der Hagen, T.H.J.J., Boersma, B.J., 2016. Turbulence attenuation in simultaneously heated and cooled annular flows at supercritical pressure. J. Fluid Mech. 799, 505–540.

Pitman, R.L., Ensor, P., 2003. Three forms of killer whales (Orcinus orca) in Antarctic waters. J. Cetacean Res. Manag. 5 (2), 131–140.

Pitman, R.L., Perryman, W.L., LeRoi, D., Eilers, E., 2007. A dwarf form of killer whale in Antarctica. J. Mammal. 88 (1), 43–48.
Rogers, M., 2019. The great white shark. Retrieved from Shark Sider: https://www.sharksider.com/great-white-shark/.
Stevens, M., Merilaita, S. (Eds.), 2011. Animal Camouflage: Mechanisms and Function. Cambridge University Press, New York.
Svendsen, M.B., Domenici, P., Marras, S., Krause, J., Boswell, K.M., Rodriguez-Pinto, I., Wilson, A.D., Kurvers, R.H., Viblanc, P.E., Finger, J.S., Steffensen, J.F., 2016. Maximum swimming speeds of sailfish and three other large marine predatory fish species based on muscle contraction time and stride length: a myth revisited. Biology open 5 (10), 1415–1419.
Valentine, J.W., 1978. The evolution of multicellular plants and animals. Sci. Am. 239 (3), 140–159.
Vincent, J.F., Mann, D.L., 2002. Systematic technology transfer from biology to engineering. Philos. Trans. R. Soc. London, Ser. A: Mathematical, Physical and Engineering Sciences 360 (1791), 159–173.
Wiirsig, B., Cipriano, F., Wiirsig, M., 1991. Dolphin movement patterns: information from radio and theodolite tracking studies. In: Dolphin Societies: Discoveries and Puzzles, pp. 79–111.
Wikipedia, 2012, August. Range of Giant Oceanic Manta Ray. Retrieved from. https://en.wikipedia.org/wiki/Manta_ray.